

MODELING METAMORPHISM IN COLLISIONAL OROGENS INTRUDED BY MAGMAS: II. FLUID FLOW AND IMPLICATIONS FOR BARROVIAN AND BUCHAN METAMORPHISM, SCOTLAND

T. LYUBETSKAYA and J. J. AGUE

Department of Geology and Geophysics, Yale University, P.O. Box 208109, New Haven, Connecticut 06520-8109, USA; jay.ague@yale.edu

ABSTRACT. This paper presents the results of two-dimensional numerical modeling of crustal fluid flow in a collisional overthrust setting during emplacement of syn-metamorphic mafic sills. An important feature of the fluid flow in the presence of magmatic intrusions is the long-lived prograde up-temperature (up-T) flow of fluid. This upward flow is driven by dehydration reactions in the rocks underlying the intrusions and upward is the consequence of the inverted thermal profile that appears within the depth range of magmatism. If magma is intruded at mid-crustal depths following crustal collision, the up-T flow regime may persist for as much as 5 Myr. Such long-lived up-T fluid flow is not observed in models without magmatism. Strong retrograde reactions in rocks surrounding intrusions may give rise to downward up-temperature flow into the heated but rapidly cooling areas of the crust during exhumation, but the fluid fluxes in these areas are typically small. The total time-integrated fluid fluxes produced by magmatism and crustal overthickening in the middle and deep crust are substantial, in some cases reaching $3,000 \text{ m}^3 \text{ m}^{-2}$ over 35 Myr. Early magmatic events may give rise to fluid fluxes exceeding $1,000 \text{ m}^3 \text{ m}^{-2}$ in only 1 Myr. The strong dehydration that accompanies the emplacement of hot magma into the relatively low-temperature wall rock leads to hydrofracturing of large volumes of crustal rocks surrounding intrusions. The fractured rock region may extend over tens of kilometers from the zone of magma emplacement. More hydrofracturing is predicted for the middle and deep crust than for the shallow crust because of the exponential decrease of crustal permeability with depth that is assumed in our models. Endothermic dehydration, exothermic retrograde hydration, and the latent heat of wall rock fusion can all influence thermal budgets. In the final part of the paper we integrate the results of the fluid flow modeling presented here, the reconstructions of thermal evolution presented in Part I, and field-based data for the type locality of Barrovian and Buchan metamorphism in Scotland. Many key phenomena predicted by our numerical models are observed in the Scottish Dalradian, including the very short thermal peaks attained over a relatively narrow time span across a broad range of metamorphic zones; penecontemporaneous Barrovian, Buchan, and granulite facies metamorphism; steep Metamorphic Field Temperature Gradients (MFTGs) in the vicinity of intrusions; and petrological evidence consistent with up-temperature fluid flow. Our results suggest that some controversial aspects of regional metamorphism in the Scottish Dalradian, including heat transfer processes and the steep MFTGs, may be plausibly explained by the effects of plutonism.

INTRODUCTION

An important aspect of syn-metamorphic magmatism within orogenic collisional terranes is the potential influence of intrusions on the patterns of crustal-scale fluid flow. The direction of fluid flow during regional metamorphism has remained as an important and controversial issue for many years (see Walther and Orville, 1984; Etheridge and others, 1984; Connolly and Podladchikov, 2007; Connolly, 2010). Inverse geochemical and petrological modeling of field and laboratory observations of metamorphic rocks has produced divergent conclusions regarding the directions of large-scale regional metamorphic flow. In particular, the prograde loss of CO_2 recorded in metasedimentary rocks in New England (Baumgartner and Ferry, 1991; Ferry, 1992), as well as oxygen isotope data in several geologic localities (Dipple and Ferry, 1992), have been interpreted as indicators of sub-horizontal fluid flow in a

direction of increasing temperature. Other studies argued that these geochemical systematics may not require up-temperature (up-T) flow, if diffusion, mechanical dispersion, and/or advection of H₂O and CO₂ across metasedimentary layers were important (Ague and Rye, 1999; Evans and Bickle, 1999; Ague, 2000). Recent three-dimensional inversions of field-based reaction progress and isotopic data suggest that metamorphic fluid flow may be highly variable, including both up-temperature and down-temperature regimes, but is generally upward on a large scale (Wing and Ferry, 2002, 2007). Forward numerical models of crustal-scale fluid flow indicate that the predominant regime of prograde flow in the middle and lower crust is upward, in the direction of decreasing temperature, and that the sub-horizontal, up-T regime of prograde fluid flow is unlikely (Hanson, 1997; Lyubetskaya and Ague, 2009a). None of the numerical models, however, have considered magmatic activity and its effect on fluid flow patterns, despite the fact that the up-temperature flow suggested by some inverse studies coincided with areas of syn-metamorphic plutonism (for example, Wing and Ferry, 2002, 2007).

This paper presents the fluid flow-related aspects of our two-dimensional (2-D) forward numerical models of regional metamorphism with syn-metamorphic magmatism (see Part I of this paper for discussion of the purely thermal aspects of the modeling). Thermal perturbations produced by magmatism and by the thermal relaxation of overthickened crust trigger metamorphic hydration and dehydration reactions within the model crustal section. We analyze the controls that sources and sinks of fluid formed by metamorphic reactions exert on the large-scale patterns of crustal fluid flow, as well as on the time-integrated fluid fluxes and fluid pressures. In cases when fluid pressures exceed lithostatic pressures due to intensive devolatilization in the vicinity of magmatic intrusions, our models simulate the process of hydrofracturing by means of iterative permeability and porosity increases. In addition, the models assess the effects that metamorphic reactions, the flow of fluid and partial melting may have on the thermal history of crustal rocks. We conclude the paper by exploring the implications that our reconstructions of thermal evolution (Part I) and of fluid flow (Part II) have for Barrovian and Buchan metamorphism in Scotland.

Our models do not account for the evolution of porosity and permeability in response to the deformation of rock matrix except for the cases of hydrofracturing. Deformation of rock matrix and porosity evolution should be greatest during crustal collision and overthrusting, which are accompanied by collapse of porosity and the expulsion of fluid from the buried rocks in the underlying plate (compare Koons and Craw, 1991). Our simulations, however, consider only the post-deformational evolution of a model orogen, when the porosity-permeability structure within the thickened crust section is likely to have equilibrated to a certain temporal and spatial average. Such an average empirical depth-dependence profile of permeability proposed by Manning and Ingebritsen (1999) is used in our modeling as the reference permeability structure (Appendix, Part I). We assume that a fixed interconnected porosity-permeability structure is maintained within the entire continental crust.

Clearly, the flow patterns and fluid fluxes are strongly dependent on the model reference permeability-depth relationship. Other relationships could yield significantly different systematics. Nonetheless, the results below predict how a representative amagmatic flow model based on the reference permeability structure will be affected by perturbations in the thermal regime caused by magmatism. We argue that these predictions, in turn, have important implications for interpreting infiltration-driven reaction progress in field settings.

The above approach, characterized by a non-deformable rock matrix, interconnected porosity, and time-invariant permeability throughout the continental crust (except for hydrofracturing), provides the most advantageous environment for the

unrestricted flow of fluid. Our models, therefore, present a boundary case for exploring possible convective and downward fluid flow in the middle and deep crust in response to syn-metamorphic magmatism and prograde devolatilization. Of course, anisotropic permeability due to metamorphic foliations, permeability heterogeneities such as low-permeability barriers to flow, and porosity and permeability evolution due to volume changes attending metamorphic reactions may all exert strong controls on fluid motion. Depending on their orientation and spatial distribution, these geologic factors can channelize or focus flow at the regional scale, as well as introduce considerable horizontal components to the fluid motion (Lyubetskaya and Ague, 2009a). Nonetheless, in prograde settings involving fluid production, available model results indicate that any sub-horizontal flow would be dominantly down-temperature, and that large-scale convective motion into regions undergoing prograde reaction is unlikely (Lyubetskaya and Ague, 2009a). On the other hand, these models do predict non-trivial downward flow into the upper crustal section when high-grade rocks exhumed from depth absorb fluid during retrograde hydration (see below).

As pointed out in Part I, the assumption of a rigid, non-compacting rock matrix is a major simplification that has important implications for flow directions. However, if compaction due to pore space collapse occurs predominantly in the vertical direction, then fluid flow will have a strong upward component. This simply reinforces earlier conclusions that flow is predominantly upward in post-collisional prograde settings (Hanson, 1997; Lyubetskaya and Ague, 2009a). We note, however that localized downward and/or lateral flow has been predicted for some compaction scenarios in the vicinity of strong heterogeneities such as shear zones (Connolly, 2010). Importantly, as fluids play a relatively minor role in the regional heat transport, the model thermal evolution and P-T-t paths are not strongly dependent on the details of the fluid flow regime, at least within the parameter space explored in our models.

MODEL FORMULATION

The numerical formulation used in this work is described by Lyubetskaya and Ague (2009a) and Part I of this paper. The model solves a system of partial differential equations that include energy conservation, mass conservation, and Darcy's law (momentum conservation) for compressible fluid using the finite difference method (Appendix, Part I). The numerical grid spacing for most of the simulations is 0.5 km in the vertical dimension and 2 km in the horizontal. Consequently, the models do not attempt to resolve any sub-grid-scale (≤ 2 km) complexities in fluid flow patterns that might arise. The model geometry is shown in figure 1.

The model of syn-metamorphic magmatism in our work is rooted in the concept of the crustal "hot zone" proposed by Annen and Sparks (2002) and Annen and others (2006). Our default model configuration includes ten individual mafic sills with a thickness of 500 m emplaced randomly within the depth range of 15 to 35 km ("mid-crustal intrusion") or 35 to 50 km ("deep intrusion"). The total thickness of intruded sills is thus 5 km; their lateral dimensions vary in a random way between 10 and 50 km. In the default case, the emplaced magma is accommodated by vertical downward displacement of the rock column that underlies the intrusion. Such vertical movement leads to crustal thickening and may produce inflexions in the intrusions within the moving rock column (see fig. 2 in Part I). We also consider an alternative model that assumes a volume-for-volume replacement of wall rock by intruded magma. The default model uses a mafic sill composition and the emplacement temperature of 1200 °C. The timing of the magmatism is 0, 5 or 15 Myr after the start of the simulation. The sills are emplaced either: a) every 20,000 years ("fast intrusion" at a rate of 2.5 cm yr⁻¹) or b) every 200,000 years ("slow intrusion" at a rate of 0.25 cm yr⁻¹). The total simulation time in these models—35 Ma—is given by the time needed for the removal by erosion of an average crustal thickness of 35 km at an exhumation rate of 1 mm yr⁻¹.

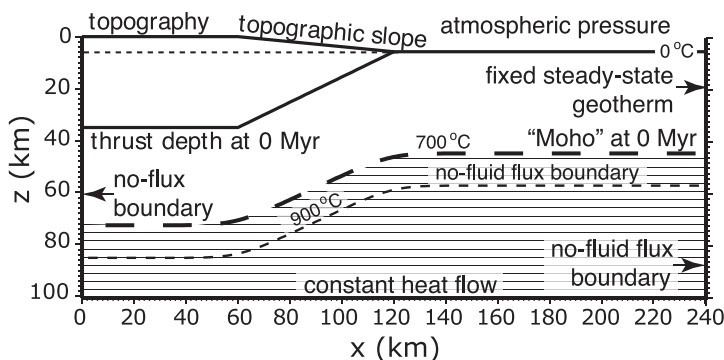


Fig. 1. Model geometry illustrating some important initial and boundary conditions. Surface held at atmospheric pressure and 0 °C for all model times. Model “Moho” is defined by the 700 °C isotherm. Below this depth, rocks contain no structural water bound in hydrous minerals (horizontal ruled area). There are no fluid fluxes across the boundaries at $x = 0$ km and $x = 240$ km, or across the 900 °C isotherm. No heat fluxes are allowed across the boundary at $x = 0$ km; the boundary at $x = 240$ km has T fixed by the steady-state geotherm. Constant mantle heat flux ($35 \cdot 10^{-3} \text{ W m}^{-2}$) prescribed at $z = 100$ km. See Part I for discussion.

The model crustal section is assumed to have an average aluminous metapelitic composition (Powell and others, 1998; see Part I). The initial water content for the crustal rocks is modeled as a function of the initial temperature distribution, based on a 5 weight percent upper limit for the chemically-bound water supply. Rocks at temperatures below 400 °C are fully hydrated, whereas the initial water content of rocks at $T > 400$ °C drops linearly from 5 weight percent at 400 °C to zero at 700 °C. The direction of the metamorphic hydration/dehydration reaction is determined by the sign of the temperature change in a rock; dehydration occurs during heating, whereas hydration occurs during cooling of a rock unit volume (Appendix, Part I).

The progress of reaction in a model rock depends on its content of the chemically-bound water. Dehydration is allowed to proceed while the rock’s bound water content is above zero; the reaction stops when the water is exhausted by devolatilization. The pore space of crustal rocks is assumed to be always filled with fluid available for hydration reactions; hydration is allowed to proceed until the upper limit for the bound water content, 5 weight percent, is attained. In addition, we consider an alternative scenario in which no hydration reactions occur during rock cooling. Metamorphic reactions within the intruded sills are not included.

We ran a series of special simulations in which fluid was consumed by partial melting and/or magmatic sills exsolved water during crystallization. However, these are small fluid sources/sinks compared to the devolatilization budget and, furthermore, their contributions tend to cancel. Consequently, they do not noticeably affect the thermal evolution or the overall time-integrated fluid fluxes, and are not illustrated in the models presented here (see table 1 for the list of simulations).

The rock permeability within the model crustal section decreases exponentially with depth with the characteristic length scale of 2.5 km, from the surface value of 10^{-16} m^2 to the reference background value of 10^{-19} m^2 . The latter is based on the empirical integrated estimate of permeability for the middle and deep crust proposed by Manning and Ingebritsen (1999). The permeability above 700 °C decreases exponentially with increasing temperature from 10^{-19} at 700 °C to $\sim 10^{-21} \text{ m}^2$ at 900 °C. As a result, the igneous rock within the intrusions and any surrounding metapelitic rocks that contain partial melt become much less permeable for fluid flow than fully crystallized rock. We adopt this conservative convention as a first approximation

TABLE 1
Variations of model parameters explored in numerical experiments

Number of sills and total thickness of intrusions	Rates of emplacement	Depth range of emplacement	Time of emplacement	Parameter variations
10 sills 0.5 km thick; 5 km (default)	0.25 cm yr ⁻¹ ("slow") 0.5 cm yr ⁻¹ 1.0 cm yr ⁻¹ 2.5 cm yr ⁻¹ ("fast")	15-35 km ("mid-crustal") 35-50 km ("deep")	0 Myr 3.33 Myr 5 Myr 10 Myr 15 Myr	Magma intrusion with / without wall rock displacement (Parts I, II) Erosion rates 0.5, 1.0, 1.5, 5.0 mm yr ⁻¹ (Parts I, II) Sill lateral dimensions 10-50 km or 6-10 km (Part I) Emplacement temperature 1200°C or 850°C (Part I) Retrograde reaction present / absent (Part II) Reaction enthalpy >0, >0, or =0 (Part II) Fusion enthalpy >0 or =0 (Part II) Basal heating below the thrust: 35, 70, or 105 mW m ⁻² (Part II) Different random configurations of individual sill depth and dimensions (not shown) Fluid exsolution from magmas/fluid consumption by crustal melts (discussed in Part II)
3 sills 1 km thick; 3 km				
6 sills 0.5 km thick; 3 km				
6 sills 1 km thick; 6 km				
5 sills 2 km thick; 10 km				
10 sills 1 km thick; 10 km				
20 sills 0.5 km thick; 10 km				

because relatively little information currently exists regarding aqueous fluid infiltration into magmatic systems. Partial melt generated in the metapelites is assumed to stay in place and does not migrate, as would be the case for *in situ* migmatite formation. We use data from Annen and Sparks (2002) and Annen and others (2006) to calculate the variations in melt fraction with temperature for igneous rocks and for metapelites (see Appendix, Part I). The model does not include any partial melting below the model crust-mantle boundary.

Rock hydrofracturing occurs when fluid pressure increases above the critical value, which is the sum of lithostatic burden of the rock column and the tensile strength of the rocks (0.01–0.03 GPa; 0.01 in our models). Hydrofracturing of rock as a result of fluid production during metamorphism is well documented from field observations and laboratory measurements (for example, Ague 1994; Flekkøy and others, 2002; Miller and others, 2003). We simulate hydrofracturing by transient porosity-permeability increases within the rocks that have fluid pressures above the critical value (Lyubetskaya and Ague, 2009a). The minimum amount of permeability production in rocks with temperatures below solidus (~ 720 °C) is determined by means of iterative adjustment of permeability, porosity, and corresponding fluid flux values, until fluid pressure is brought just below the critical value. Permeability is generally thought to have a power-law dependence on porosity; we employ the expression of Walder and Nur (1984) to describe permeability (k_ϕ) as a function of changes in porosity (ϕ):

$$k_\phi = k_{\phi_0} \left(\frac{\phi^n - \phi_{\min}^n}{\phi_0^n - \phi_{\min}^n} \right), \quad (1)$$

where k_{ϕ_0} is the reference permeability defined by the depth-dependent permeability curve described in Part I and ϕ_0 is the reference porosity for the flow region ($5 \cdot 10^{-4}$; Connolly, 1997; Hiraga and others, 2001). The minimum porosity $\phi_{\min} = 10^{-6}$ corresponds to the probable minimum necessary to maintain an interconnected pore network (Bickle and Baker, 1990). The exponent n typically takes on values between 2 and 3; 2 is used herein but other values would not change our interpretations significantly.

Adjustments of permeability, porosity, and fluid pressure are done numerically over the time span of a single time step and are returned to the reference values at the beginning of the next time step, as hydrofracturing and the relaxation of permeability after hydrofracturing events probably occur on rapid timescales as short as 10^3 years or even less (compare Sleep and Blanpied, 1992; Ague and others, 1998; Ingebritsen and Manning, 2010). The above procedure is repeated for succeeding time steps if fluid pressures exceed the critical value. We emphasize that a rigorous treatment of hydrofracturing would need to consider in detail the rheology of the rock mass undergoing brittle failure as well as post-hydrofracturing compaction and the resultant changes in porosity and permeability. Our results, however, do provide useful perspectives on the potential regional extent of hydrofracturing, and whether or not this process is likely to be important in systems intruded by magmas.

RESULTS

Fluid Flow in the Presence of Magmatism

The patterns of fluid flow that arise in a collisional orogen during post-deformational metamorphism in the absence of magmatic intrusions have been explored in another paper (Lyubetskaya and Ague, 2009a). In agreement with earlier numerical modeling of metamorphic fluid flow in such settings (Hanson, 1997), the predominant deep crustal flow regime during prograde metamorphism at likely values

of rock permeability was found to be toward the surface, in the direction of decreasing temperature. A limited occurrence of upward, up-temperature (up-T) prograde fluid flow in the uppermost part of the lower plate of the thrust is observed at early stages (1-3 Myr) of model thermal evolution in the presence of the inverted thermal profile within the doubled crustal section. Such flow is generated by dehydration reactions in the lower plate of the thrust. The fluid expelled by deep rocks is pushed upward toward the surface through the area of increased temperature, but the time-integrated fluid fluxes are only about $100 \text{ m}^3 \text{ m}^{-2}$ over 2 Myr. It is possible that larger up-T fluxes could be generated during the collisional stage if plate convergence and, thus, an inverted geotherm, were protracted. The feasibility of this scenario deserves further investigation; however, we focus herein on the post-collisional history.

Retrograde hydration reactions may give rise to up-T flow away from the surface and toward the area of intensive fluid consumption (Lyubetskaya and Ague, 2009a; retrograde flow is not considered by Hanson, 1997). In particular, rocks in the upper 10 to 20 km of the crust that undergo retrograde cooling and hydration on their ascent to the surface during exhumation may draw fluid downward from the surface. The existence of such downward, up-T fluid flow is consistent with a number of field observations (Yakovlev, 1993; Stober and Bucher, 2004).

The major features of fluid flow characteristic for amagmatic regional metamorphism are also observed in models with syn-metamorphic intrusions, but considerable differences are also evident. The initiation of magmatism produces dramatic perturbations in crustal thermal structure. In particular, early magmatism (at 0 Myr or 5 Myr) at mid-crustal depths tends to generate a long-lived inverted geotherm that may be preserved for 3 to 5 Myr after the end of intrusion (fig. 2A, B). During thermal relaxation of the inverted geotherm, rocks that lie beneath the magmatism region are rapidly heating and dehydrating, producing large quantities of fluid. A considerable fraction of the resulting fluid flow is directed upward, into the area of hydration that appears within the cooling rocks surrounding the magmatic intrusions and further towards the surface. Such sub-vertical flow persists in most of the thickened crust segment of the model during the whole period of the relaxation of the inverted geotherm, and further on until the end of the simulation. This model, therefore, predicts an environment where relatively long-lived up-T fluid flow can occur; but in the absence of magmatism, such flow is only observed at the earliest stages of the exhumation history in the region of the inverted geotherm.

A considerable fraction of the up-T flow is in the retrograde area, which comprises the high-temperature zone of magmatism that undergoes cooling during post-magmatic relaxation (fig. 2A, B). Even though the flow is retrograde, temperatures are still high such that upper greenschist and amphibolite facies mineral assemblages could develop after the thermal peak if retrograde reaction was extensive. The remaining fraction of the up-T flow is within the rocks beneath the magmatism zone that are continuously heating up, that is in the prograde area of the model crust below the fault zone.

Similar patterns of fluid flow arise in simulations with intrusions emplaced at deeper levels of the thickened crustal section early in the model evolution at 0 Myr or 5 Myr (fig. 2C, D). The strong, magmatism-induced thermal anomaly develops at 30 to 55 km depth. A large part of the fluid generated in the rocks underneath the area of magmatism is moving upward, into the heated region. The fluid is partly consumed by hydration reactions and partly transferred further toward to the surface. Because the inverted thermal gradient produced by deep magmatism is not as pronounced as in the case of mid-crustal magmatism, its relaxation takes 2 to 4 Myr; this corresponds to a shorter history of up-T prograde fluid flow than in the model with early mid-crustal magmatism (fig. 2A, B).

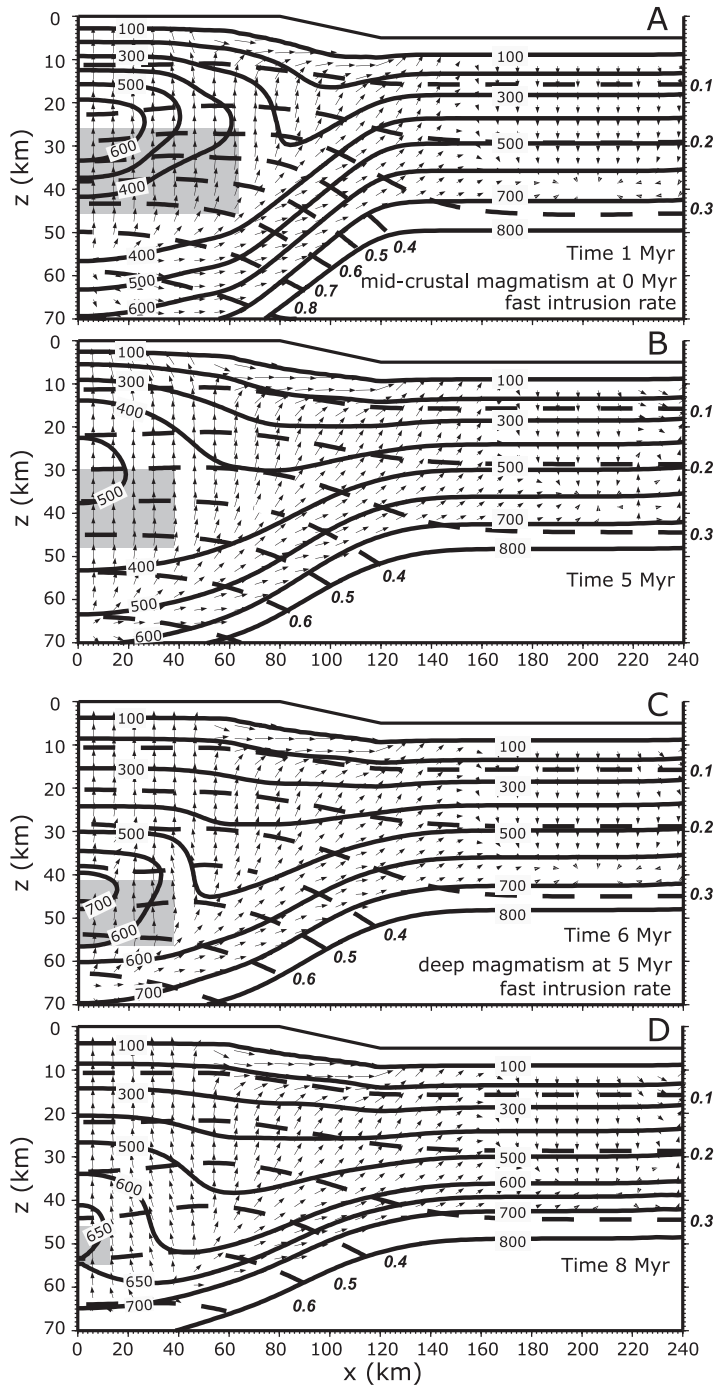


Fig. 2. Model thermal field ($^{\circ}\text{C}$, solid lines), fluid pressure (GPa, dashed lines, values in italics) and fluid mass flux (arrows; length of arrows is scaled for visibility with logarithmic scale; mass flux in the upper 5 km is not shown). Regions dominated by up-T flow shown with gray shading. (A) Results at 1 Myr for erosion rate 1 mm yr^{-1} and 10 basaltic sills 500 m thick intruded every 20 kyr in the depth interval of 15–35 km beginning at 0 Myr. Note large region of up-T flow extending from $x = 0 \text{ km}$ to $\sim 60 \text{ km}$ at depths of about 25–45 km. (B) Same as A, at 5 Myr. (C) Results at 6 Myr for erosion rate 1 mm yr^{-1} and 10 basaltic sills 500 m thick intruded every 20 kyr in the depth interval of 35–50 km beginning at 5 Myr. (D) Same as C, at 8 Myr.

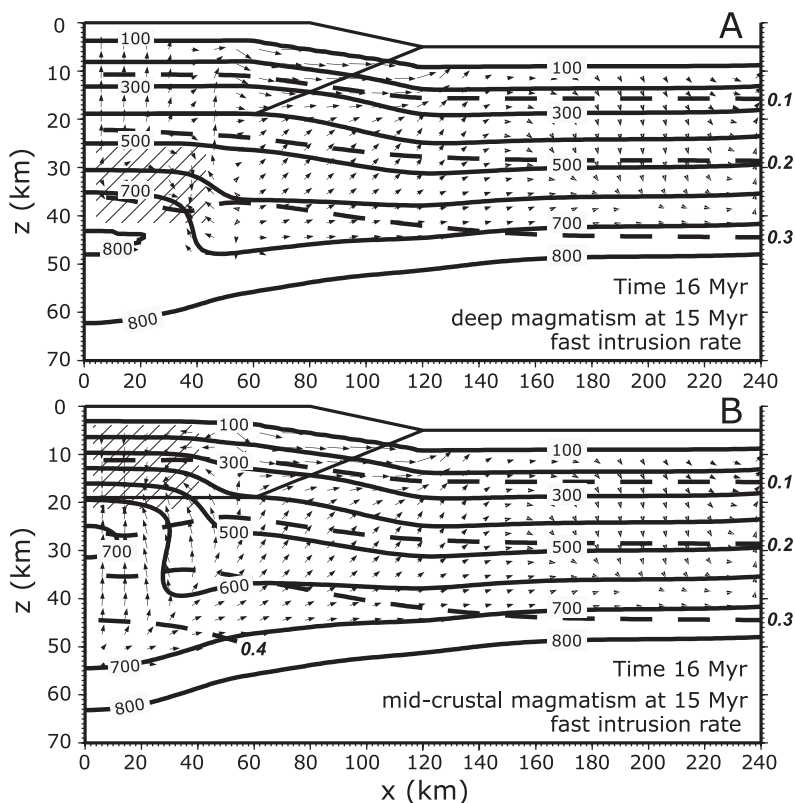


Fig. 3. Model thermal field ($^{\circ}\text{C}$, solid lines), fluid pressure (GPa, dashed lines, values in italics) and fluid mass flux (arrows; length of arrows is scaled for visibility with logarithmic scale; mass flux in the upper 5 km is not shown). Diagonal rule pattern denotes the areas of up-temperature downward fluid flux in the overthrust region. (A) Results at 16 Myr for erosion rate 1 mm yr^{-1} and 10 mafic sills 500 m thick intruded every 20 kyr in the depth interval of 35–50 km beginning at 15 Myr. (B) Results at 16 Myr for erosion rate 1 mm yr^{-1} and 10 mafic sills 500 m thick intruded every 20 kyr in the depth interval of 15–35 km beginning at 15 Myr.

When deep intrusion is initiated at a later time in the exhumation history, high temperatures develop in the lower crust, but there is little or no inversion of thermal gradients (fig. 3A). Correspondingly, no significant up-T prograde flow is observed in such models. For mid-crustal magmatism that starts at 15 Myr, the crust is considerably reduced in thickness due to erosion, and the inverted geotherm is relatively short-lived (fig. 3B). Up-T flow is present, but is not as intensive as in the cases with early intrusions. These relationships reflect the lower rates of fluid production and lesser amount of bound water available for dehydration in the rocks beneath the magmatic zone (their bound water content being on average 1 wt% or less). Larger upward, up-T fluxes beneath and to the sides of intrusions would be expected, however, if the intrusion depth was shallower ($\sim 5\text{--}15 \text{ km}$), as the wall rocks would not be as hot and would have more water available for devolatilization (not illustrated).

Retrograde, downward up-T flow in models with syn-metamorphic intrusions, as in the overthrust models in the absence of magmatism, may develop within the rocks with elevated but decreasing temperatures away from the areas of strong prograde fluid sources (Lyubetskaya and Ague, 2009a). A characteristic example of such downward retrograde flow is visible in figure 2 on the flank of the model thrust ($x \gtrsim$

160 km), although the fluid fluxes in this area are extremely small, $\sim 10 \text{ m}^3 \text{ m}^{-2}$ over 35 Myr. In contrast, the zone of hydration in the core of the thrust in the models illustrated in figure 2 does not initiate downward flow because of the strong influx of fluid liberated from dehydrating rocks underneath the magmatic region. Downward, up-T flow driven by hydration of the cooling rocks around the magmatic bodies generally arises at later times, when the intensity of fluid sources is diminished and the amount of bound water available for dehydration in the deep rocks is reduced (fig. 3A, B). Such flow, however, is generally short-lived and dependent on the availability of anhydrous minerals within the cooling rocks. It must also be noted that our models incorporate a non-collapsing, interconnected porosity for the bulk of the crustal section, thus providing the most favorable scenario for downward circulation of fluid. In models that take into account the deformation of rock matrix in response to fluid pressures that are less than lithostatic, the downward flow of fluid that appears in our models within the mid-crustal and deep rocks may be prevented by the collapse of pore space due to fluid pressure decreases related to hydration reactions. Nonetheless, such flow is likely to persist in the shallow crust to 5 to 10 km depth in rocks that are sufficiently strong to maintain interconnected porosity.

Fluid Fluxes

The time-integrated fluid fluxes attained in the models with syn-metamorphic intrusions are substantial, especially when magmatism begins early after the start of exhumation. Figure 4 illustrates the temporal evolution of time-integrated fluxes in a model of regional metamorphism with erosion rate of 1 mm yr^{-1} in the absence of magmatism. These flux values are for the total amount of fluid flow—both prograde and retrograde—through a given rock parcel. At 10 Myr in the model exhumation history, only a relatively small volume of deeper rocks within the core of the thrust attain fluxes on the order of $1,000 \text{ m}^3 \text{ m}^{-2}$ (fig. 4B). Higher fluid fluxes are recorded only in the uppermost parts of the crust above 10 km, where permeability is larger by as much as two orders of magnitude relative to the background value ($k_{\phi 0} = 10^{-19} \text{ m}^2$) and there is a strong component of topographically-driven flow (compare Garven and Freeze, 1984).

The incorporation of magmatic intrusions can lead to a substantial increase in the rates of fluid production. In figure 5 we plot the volumetric fluid fluxes for models with mid-crustal and deep mafic magmatism initiated at 0 and 5 Myr. For the 0 Myr case, the amount of fluid released after 1 Myr of simulation (fig. 5A, B) is much larger than that released during simple relaxation of the geotherm in the absence of magmatism (fig. 4A). The volumetric fluid fluxes in a model with mid-crustal magmatism are somewhat higher than in the deep magmatism model and may exceed $1,000 \text{ m}^3 \text{ m}^{-2}$ in 1 Myr (fig. 5A). This is a consequence of the prolonged lifetime of the inverted geotherm in this model and the correspondingly extended period of heating and strong fluid production within the lower plate of the thrust. Note the vertical linear structures in the spatial distribution of the highest fluid fluxes, particularly in figures 5A and 5B. These features generally coincide with the tips of magmatic sills. Rocks with temperatures above the solidus ($\sim 720 \text{ }^\circ\text{C}$) in our models have low permeability below the reference crustal value ($k_{\phi 0} = 10^{-19} \text{ m}^2$), which diverts the fluid flow sub-horizontally underneath the newly emplaced intrusions. It is then focused upward at the edges of the sills where the matrix permeability is larger.

For magmatism that begins at 5 Myr, a considerable amount of dehydration driven by thermal relaxation of the geotherm has already occurred prior to intrusion (compare fig. 4B). By this time the overall temperature of rocks in the model thrust section is higher than at the beginning of the simulation, and the thermal perturbations in crustal rocks produced by magmatism and the corresponding rates of dehydration reaction are not as large as in the models with early intrusions. Nonethe-

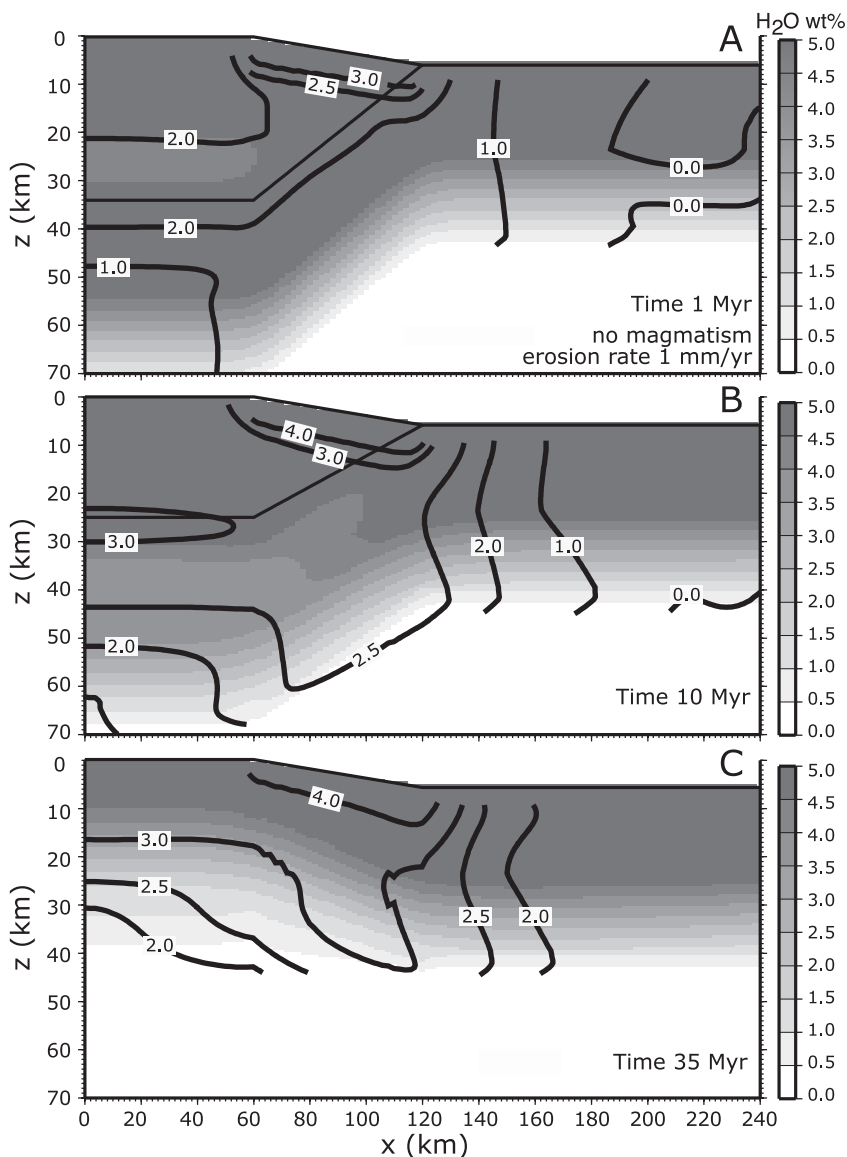


Fig. 4. Time-integrated volume fluid flux ($\log_{10} \text{m}^3 \text{m}^{-2}$, solid lines) and the amount of mineralogically-bound water in crustal rocks of metapelitic composition (weight %, shading) in the overthrust model with erosion rate 1 mm yr^{-1} in the absence of magmatism. Contours terminate at the model “Moho”. (A) Results at 1 Myr. (B) Results at 10 Myr. (C) Results at 35 Myr.

less, for a given time, the time-integrated fluxes in these models can be significantly larger than in the absence of magmatism and may exceed $1,500 \text{ m}^3 \text{m}^{-2}$ in 10 Myr for mid-crustal intrusions (compare figs. 4B and 5C).

In models with intrusion beginning at 15 Myr, the amount of fluid production initiated by magmatism is less than in the models with early magmatism due to smaller thermal effects of magmatism on relatively high-temperature rocks, slower reaction rates, and the diminished bound water supply in these models. By this time, however,

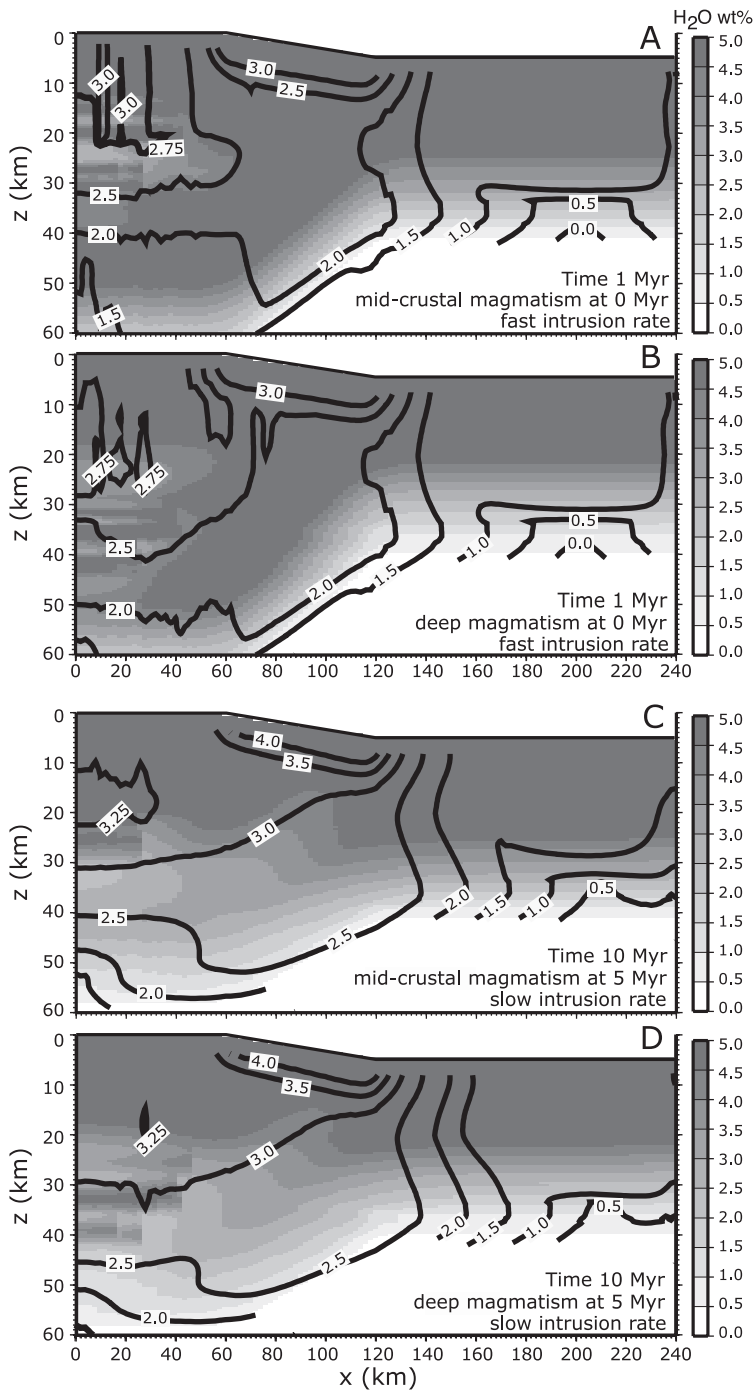


Fig. 5. Time-integrated volume fluid flux ($\log_{10} \text{m}^3 \text{m}^{-2}$, solid lines) and the amount of bound water in crustal rocks of metapelitic composition (weight %, shading). (A) Results at 1 Myr for erosion rate 1 mm yr^{-1} and 10 mafic sills 500 m thick intruded every 20 kyr in the depth interval of 15–35 km beginning at 0 Myr. (B) Results at 1 Myr for erosion rate 1 mm yr^{-1} and 10 mafic sills 500 m thick intruded every 20 kyr in the depth interval of 35–50 km beginning at 0 Myr. (C) Results at 10 Myr for erosion rate 1 mm yr^{-1} and 10 mafic sills 500 m thick intruded every 200 kyr in the depth interval of 15–35 km beginning at 5 Myr. (D) Results at 10 Myr for erosion rate 1 mm yr^{-1} and 10 mafic sills 500 m thick intruded every 200 kyr in the depth interval of 35–50 km beginning at 5 Myr.

the fluid flux component generated by regional metamorphism in response to crustal thickening becomes substantial, so that the total time-integrated fluid fluxes in the core of the thrust above 25 km exceed $1,000 \text{ m}^3 \text{ m}^{-2}$.

In all of the models, the time-integrated fluid fluxes at mid-crustal depths (below about 10 km) are generally $2,000$ to $3,000 \text{ m}^3 \text{ m}^{-2}$ by the end of the simulations. The rate of fluid production is strongly tied to the pace of intrusion, particularly for cases of early magmatism when the wall rocks still contain substantial H_2O available for dehydration. Fluxes within the shallower rocks (upper 10 km) below the topographic slope may exceed $10^4 \text{ m}^3 \text{ m}^{-2}$. These shallower fluxes, however, are dominated by topography-driven flow and reflect the very high permeability in the subsurface rocks; they are also observed in the numerical models of regional metamorphism in the absence of magmatism (fig. 4B, C). None of the simulations in the parameter space explored in this work predicted mid-crustal fluid fluxes in excess of $4,000 \text{ m}^3 \text{ m}^{-2}$, including models in which the exsolution of magmatic fluid by crystallizing sills was taken into account (not shown). The fluid fluxes in our models are therefore not large enough to noticeably affect the regional-scale thermal structure of the model crustal section. For example, the elevation of temperature by fluid advection in the area above the magmatic intrusions in figure 5A is less than 10°C .

For the models shown, the devolatilization of the rock column provides the fluid to produce the mid- and deep-crustal time-integrated fluid fluxes. Critically, there are no external fluid sources; for example, the rock beneath the model “Moho” only contains anhydrous mineral assemblages and cannot produce fluid (fig. 1; Appendix, Part I). The initial porosity ($5 \cdot 10^{-4}$) for all models is fully saturated. If this pore space was allowed to collapse, then it could yield an additional source of fluid that is not considered in our models. However, the amount of fluid would be small. For a 70 km-thick column of crust that underwent complete collapse to produce vertical flow, the time-integrated flux out of the top of the column would be $70,000 \text{ m}^3 \cdot 5 \cdot 10^{-4} \text{ m}^3 \text{ m}^{-3} = 35 \text{ m}^3 \text{ m}^{-2}$. This value is trivial compared to the fluid fluxes generated by devolatilization.

Hydrofracturing

Intensive devolatilization within the fast heating rocks surrounding the freshly emplaced mafic sills commonly leads to the elevation of fluid pressures above the lithostatic values. Our models simulate the process of hydrofracturing in crustal rocks at pressures exceeding the lithostat by iterative increases in rock permeability and porosity. Figure 6 illustrates the crustal permeability structure produced by hydrofracturing during magmatism at the “fast” intrusion rate. The earliest thermal pulses trigger very rapid devolatilization that elevates fluid pressure in a large region of the model crust section. The effect may be manifested at distances of more than 20 km from the actual depth of sill emplacement. The permeability of the fractured rocks increases in the vicinity of intrusion. For early mid-crustal magmatism, the increase in permeability required for bringing the fluid pressures below lithostatic values at short distances from the sills may reach two orders of magnitude (fig. 6A). The area of hydrofracturing contracts with time and permeability in the fractured zone drops, as thermal conduction reduces temperature gradients in the model crustal section and the rates of dehydration correspondingly diminish (fig. 6B). The model permeability of wall rocks is lower around deep intrusions and, thus, fracturing may affect greater volumes of deep rocks (fig. 6C, D).

In all of the models, hydrofracturing occurs predominantly within the mid-crustal and deep rocks, below 20 km depth; this is explained by the depth-dependence of rock permeability with its exponential increase toward the surface. Yardley (2009) has argued that fracturing is uncommon in shallow contact aureoles (although we note that many magmatic-hydrothermal ore deposits are highly fractured). The relatively

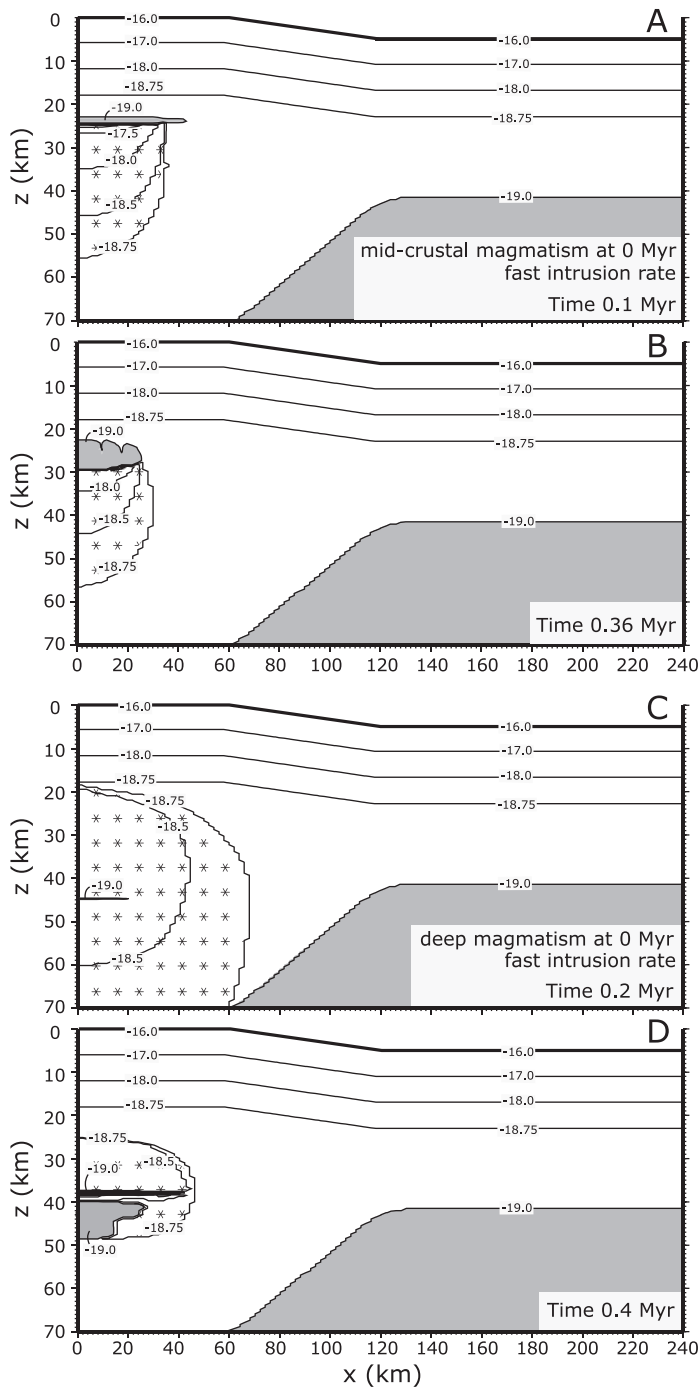


Fig. 6. Crustal permeability structure ($\log_{10} \text{ m}^2$, solid lines). Hydrofractured regions shown with asterisk pattern. Shading denotes the rocks with permeability below the reference deep crustal value, 10^{-19} m^2 (k_d drops from 10^{-19} at 700°C to $\sim 10^{-21} \text{ m}^2$ at 900°C). (A) Results at 0.1 Myr for erosion rate 1 mm yr^{-1} and 10 mafic sills 500 m thick intruded every 20 kyr in the depth interval of 15–35 km beginning at 0 Myr. (B) Same as A, at 0.36 Myr. (C) Results at 0.2 Myr for erosion rate 1 mm yr^{-1} and 10 mafic sills 500 m thick intruded every 20 kyr in the depth interval of 35–50 km beginning at 0 Myr. (D) Same as C, at 0.4 Myr.

high permeability in the upper crust may help to explain the limited occurrence of fractures in some contact zones of shallow magmatic intrusions. On the other hand, middle and deep crustal rocks will tend to have lower permeabilities and, thus, be much more prone to high fluid pressures and hydrofracturing during prograde devolatilization.

When magmatism is initiated at later times in the model history, the amount of pressure elevation and the corresponding extent of hydrofracturing are generally less than in models with early magmatism, due to the smaller thermal contrast driving dehydration reactions. Even then, the zone of hydrofracturing may extend to 10 to 15 km from the depth of intrusion in models with magmatism starting at 5 Myr, and to up to 5 km in models with magmatism starting at 15 Myr (not shown). In summary, the models predict that hydrofracturing can occur at great distances from the sites of intrusion. This result poses a challenge for determining the causes of hydrofracturing in field settings, because the magmatic bodies may be far removed from their associated fracture zones.

Thermal Effects of Metamorphic Reactions and Partial Melting

The dramatic perturbations of crustal thermal structure produced by magmatic intrusion give rise to the development of intensive metamorphic reaction within crustal rocks. Metamorphic hydration and dehydration reactions are strongly dependent on the rates of temperature change in a system (Ridley, 1986; Lutge and others, 2004, and references therein). Thermal pulses related to magmatism lead to intensive production of fluid via endothermic devolatilization reactions in the parts of the crust that undergo heating, in particular, in the wall rock around a newly emplaced sill. On the other hand, exothermic retrograde hydration reactions occur in rocks while they undergo cooling, such as during the post-magmatic relaxation of the thermal anomaly. The enthalpies of hydration and dehydration reactions differ considerably from zero (Peacock, 1989; Connolly and Thompson, 1989) and, thus, they may noticeably affect the thermal history of metamorphosed rocks (Lyubetskaya and Ague, 2009b).

Figures 7A and 7B demonstrate the effect of reaction enthalpy on the thermal evolution of crustal rocks during syn-metamorphic intrusion of 10 mafic sills, each 500 m thick. The model P-T paths are shifted noticeably towards lower temperatures when reaction enthalpy is taken into account, in comparison to the case when the thermal effects of reaction are set to zero. The effect is greater for magmatism that starts at or soon after the beginning of simulation, at 0 or 5 Myr. In such models, magmatic intrusion leads to the development of an inverted thermal gradient; the post-magmatic relaxation of the inverted gradient results in very fast heating and strong devolatilization of the deeper rocks. The consumption of heat by dehydration reaction diminishes rock temperature by as much as 20 to 40 °C in comparison to the case with zero enthalpy during the prograde heating phase; the P-T-t paths of the two models therefore strongly diverge. When the deep rocks begin to cool on their ascent to the surface, dehydration is replaced by retrograde hydration reactions which liberate heat. Thus, the P-T-t paths of deep rocks in the two models of figures 7A and 7B will converge again. Larger reductions in peak temperatures due to decarbonation reactions may be possible for more complex lithological packages that contain metacarbonate rocks (Lyubetskaya and Ague, 2009b).

The capacity for retrograde reactions to produce heat within metamorphosed rock sections has been suggested to be an important contribution to the crustal heat budget (Haack and Zimmermann, 1996). Although in the absence of magmatism the thermal effects of hydration reactions are typically small (Lyubetskaya and Ague, 2009b), the relaxation of strong thermal anomalies produced by magmatic intrusion may lead to intensive hydration that will liberate heat and thus delay cooling of the hydrating rock. In the absence of retrograde reaction, thermal peaks corresponding to

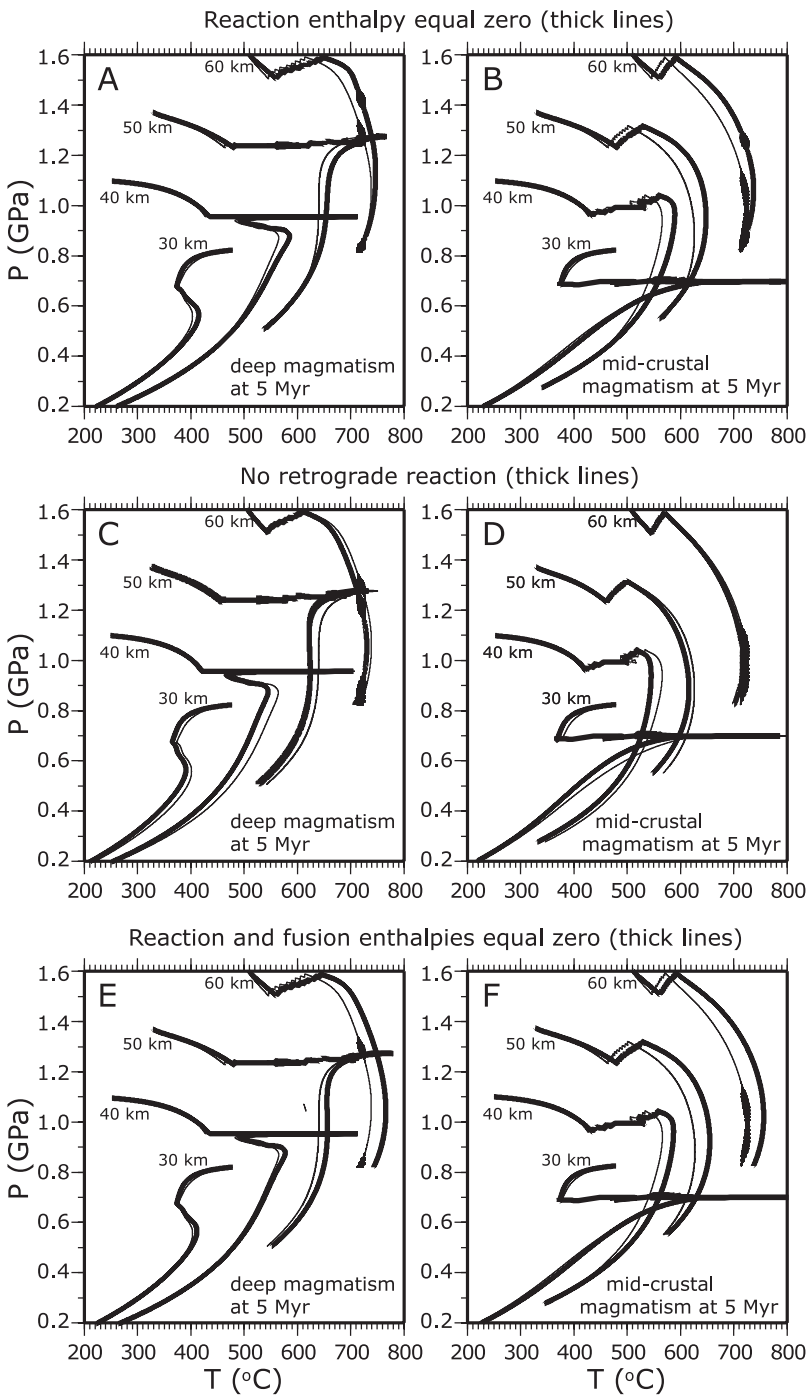


Fig. 7

magmatic intrusion tend to diffuse faster than in a model which includes hydration reactions (fig. 7C, D). The effect is especially important for early mid-crustal magmatism characterized by relatively cool wall rock and correspondingly fast relaxation of a thermal anomaly; the difference between the P-T-t paths in the two models may then exceed 30 °C. It should be noted, however, that reality lies somewhere in between the two limiting cases illustrated in figures 7C and 7D, that is, a model with hydration reaction controlled only by a rock's mineralogical capacity for retrogression and a model with no retrograde hydration. Metamorphic reactions are typically accompanied by changes in mineral volume: dehydration usually leads to the reduction of solid volume and corresponding increase of permeability, at least transiently, whereas hydration leads to increases in mineral volume, clogging of pore space and decreases in permeability (Balashov and Yardley, 1998; Zhang and others, 2000; Tenthorey and Cox, 2003). Because of the decrease in permeability, hydration in real rocks is thus likely to be terminated before all of the minerals available for hydration were processed by metamorphic reaction, unless porosity and permeability are continually created by some external process such as fracturing due to tectonic deformation. In addition, recent results indicate that hydration can drive fracturing and porosity production in some retrograde settings (Iyer and others, 2008).

The latent heat of fusion provides another heat sink in the thermal budget of crustal rocks. Partial melting of metapelitic rocks at the base of the crust and around intrusions will consume heat and thus result in lower temperatures than for the case where the latent heat of fusion is not accounted for. In figures 7E and 7F we compare the P-T-t paths for the default models of magmatism with models in which latent heats of reaction and fusion are set to zero. The total decrease in temperature due to the thermal effects of partial melting and dehydration may reach 50 °C for the deepest rocks initially at 60 km depth. These rocks are heated to temperatures above the solidus as a result of crustal thickening. The thermal effect of fusion is not as strong for shallower rocks as melting in the wall rock surrounding intrusions in our models is generally highly transient and the fraction of generated melt is small. The largest amounts of melt are observed in models with magmatism initiated late in the thrust exhumation history. In figures 8A and 8B we compare the distribution of melt produced in the models with mid-crustal and deep magmatism initiated at 15 Myr. Because of relatively high wall rock temperatures by the time of magmatism initiation, the amount of melt produced at mid-crustal depth between freshly emplaced sills may reach 15 weight percent (fig. 8A), but the volume of rock that undergoes melting is small. Note the zone of partial melting at the base of the crust resulting from crust thickening (fig. 8A). For deep magmatism, the intrusion of magma in the very hot wall rocks in the vicinity of the crust-mantle boundary generates partial melting in a larger volume of rocks. The melt fraction around newly emplaced sills in this model may

Fig. 7. Effects of heat of reaction and latent heat of fusion. Model P-T-t paths for erosion rate 1 mm yr⁻¹ and intrusion consisting of 10 mafic sills 500 m thick intruded every 200 kyr. The P-T-t paths are for the rock column located at $x = 10$ km. Initial rock depth (km) shown for each P-T-t path. Small temperature fluctuations at ~715 °C are related to the initiation or termination of partial melting in metapelitic rocks and result from the relatively sparse numerical grid and the shape of the melting function (see Appendix, Part I). (A) Magmatism in the depth interval of 35–50 km beginning at 5 Myr (thin lines); same model with metamorphic reaction enthalpy set to zero is shown in thick lines. (B) Magmatism in the depth interval of 15–35 km beginning at 5 Myr (thin lines); same model with metamorphic reaction enthalpy set to zero is shown in thick lines. (C) Magmatism in the depth interval of 35–50 km beginning at 5 Myr (thin lines); same model with retrograde hydration reaction absent is shown in thick lines. (D) Magmatism in the depth interval of 15–35 km beginning at 5 Myr (thin lines); same model with retrograde hydration reaction absent is shown in thick lines. (E) Magmatism in the depth interval of 35–50 km initiated at 5 Myr (thin lines); same model with metamorphic reaction enthalpy and latent heat of fusion set to zero is shown in thick lines. (F) Magmatism in the depth interval of 15–35 km beginning at 5 Myr (thin lines); same model with metamorphic reaction enthalpy and latent heat of fusion set to zero is shown in thick lines.

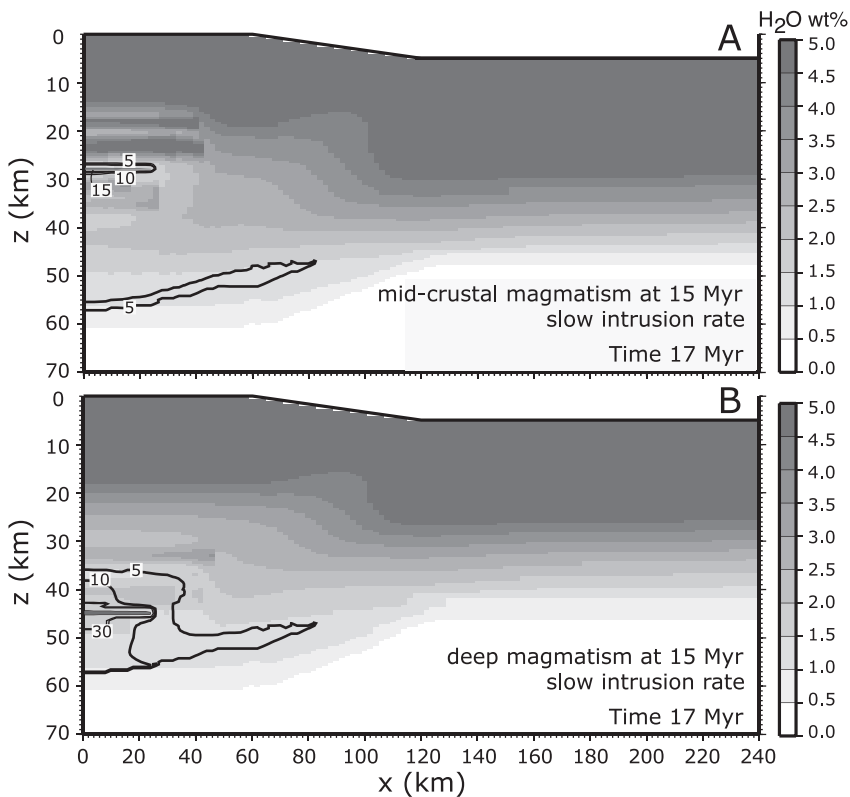


Fig. 8. Melt percent in metapelitic rocks (by mass, solid lines) and the amount of bound water in crustal rocks of average metapelitic composition (weight %, shading) for erosion rate 1 mm yr^{-1} and 10 mafic sills 500 m thick intruded every 200 kyr. Results correspond to the completion of magmatism at 17 Myr. (A) Magmatism in the depth interval of 15–35 km beginning at 15 Myr. (B) Magmatism in the depth interval of 35–50 km beginning at 15 Myr.

reach 0.3 (fig. 8B). Therefore, our models predict more crustal melting and, potentially, more extensive assimilation and/or mixing of crustal melts into mafic magmas for deep magma emplacement than for mid-crustal and shallow emplacement (compare DePaolo, 1981; Annen and others, 2006).

DISCUSSION AND IMPLICATIONS FOR BARROVIAN AND BUCHAN METAMORPHISM, SCOTLAND

Summary of Fluid Flow in the Presence of Magmatism

A noteworthy aspect of fluid flow in models with syn-metamorphic intrusions, as opposed to the models without magmatism, is the prediction of long-lived, prograde, up-temperature (up-T) flow that may persist for as much as ~ 5 Myr. Fluids generated by dehydration reactions in the deep rocks underlying magmatic intrusions move upward into the inverted thermal profile that appears within the depth range of magmatism. The time-integrated fluid fluxes for the resulting up-T, upward flow may exceed $1,000 \text{ m}^3 \text{ m}^{-2}$. The results of this study, as well as those of Hanson (1997) and Lyubetskaya and Ague (2009a), indicate that large-scale downward or sub-horizontal up-T flow at high temperatures during prograde regional metamorphism is probably rare. On the other hand, we show that upward up-T flow through the crustal rocks underlying magmatic intrusions is highly plausible. This type of flow may help explain

petrological and geochemical data consistent with prolonged histories of prograde flow in a direction of increasing temperature (Wing and Ferry, 2007).

The total time-integrated fluid fluxes produced by magmatism and crustal overthickening below 10 km depth in our models are substantial, in some cases reaching $3,000 \text{ m}^3 \text{ m}^{-2}$ over 35 Myr. Large fluxes of more than $1,000 \text{ m}^3 \text{ m}^{-2}$ may be attained over short timescales of about 1 Myr in the models with early mafic magmatism and fast emplacement rates. These fluxes, however, are still insufficient to noticeably affect the model crust thermal structure: the temperature elevation due to the fluid advection is less than 10°C in all of our models. However, if the fluid flow is focused into conduits with strongly increased permeability, such as deep fracture zones, the fluxes in such channels may lead to greater thermal effects (Chamberlain and Rumble, 1989). Furthermore, if the flow is largely focused into conduits, then the time-integrated fluxes in the conduits will be well in excess of $\sim 10^3 \text{ m}^3 \text{ m}^{-2}$. For example, if a flux of $3,000 \text{ m}^3 \text{ m}^{-2}$ was mostly focused into fractures comprising 10 volume percent of the rock, then fluxes in the conduits would approach $3 \times 10^4 \text{ m}^3 \text{ m}^{-2}$. Such fluxes are sufficient to produce considerable chemical and isotopic metasomatism in and around the conduits (for example, Ague, 1994, 1997; van Haren and others, 1996; Oliver and others, 1998; Penniston-Dorland and Ferry, 2008). Hydrofracturing is predicted to be extensive in the middle and lower crust due to low permeabilities which allow high fluid pressures to build up during devolatilization.

Summary of Model Results and the Implications for Barrovian and Buchan Metamorphism in Scotland

The thermal aspects of the modeling presented in Part I and the fluid flow characteristics discussed herein are surveyed in the context of geological and petrological data for the Barrovian and Buchan metamorphic zones in the Scottish Dalradian (Horne, 1884; Barrow, 1893). A major motivation for this effort is that Barrovian metamorphism in Scotland required additional heat sources beyond the thermal relaxation of overthickened crust of normal thermal structure (Baxter and others, 2002; Ague and Baxter, 2007). Despite the fact that our models are not intended to represent any specific geologic locality, they provide important points of comparison with field data and may be used to test existing hypotheses bearing on the development of regional metamorphism in Scotland. More detailed modeling of the Barrovian and Buchan zones in the future will require tighter, field-based constraints on the chronology of intrusion, P-T-t pathways, exhumation rates, and other critical geologic variables.

We begin by reviewing some of the major characteristics of P-T-t evolution predicted for collisional orogens lacking magmatism. The results of our modeling are consistent with earlier studies suggesting that the thermal relaxation of thickened continental crust with average values of radiogenic and basal heating in the absence of additional heat sources is unlikely to produce the high temperatures characteristic for Barrovian metamorphism at moderate pressures (for example, Jamieson and others, 1989; Huerta and others, 1996; Burg and Gerya, 2005). In the absence of magmatism, the peak temperatures (T_p) of deep and mid-crustal rocks in the overthrust setting are mostly below 650 to 700°C and are attained after 30 to 40 Myr of exhumation (fig. 9A, dashed lines). The P-T-t paths form broad curves such that rocks are maintained at temperatures close to their peak values for at least 5 to 10 Myr. There is a considerable difference in the timing of the peak (maximum) temperature attainment for rocks located at different depths (~ 5 Myr for 10 km of depth difference at an erosion rate of 1 mm yr^{-1}).

In figure 9C we plot mineral assemblages predicted to develop in metapelitic rocks at their peak thermal conditions in the overthrust model without magmatism based on the pseudosection of figure 9B (see Part I for discussion). The peak mineral

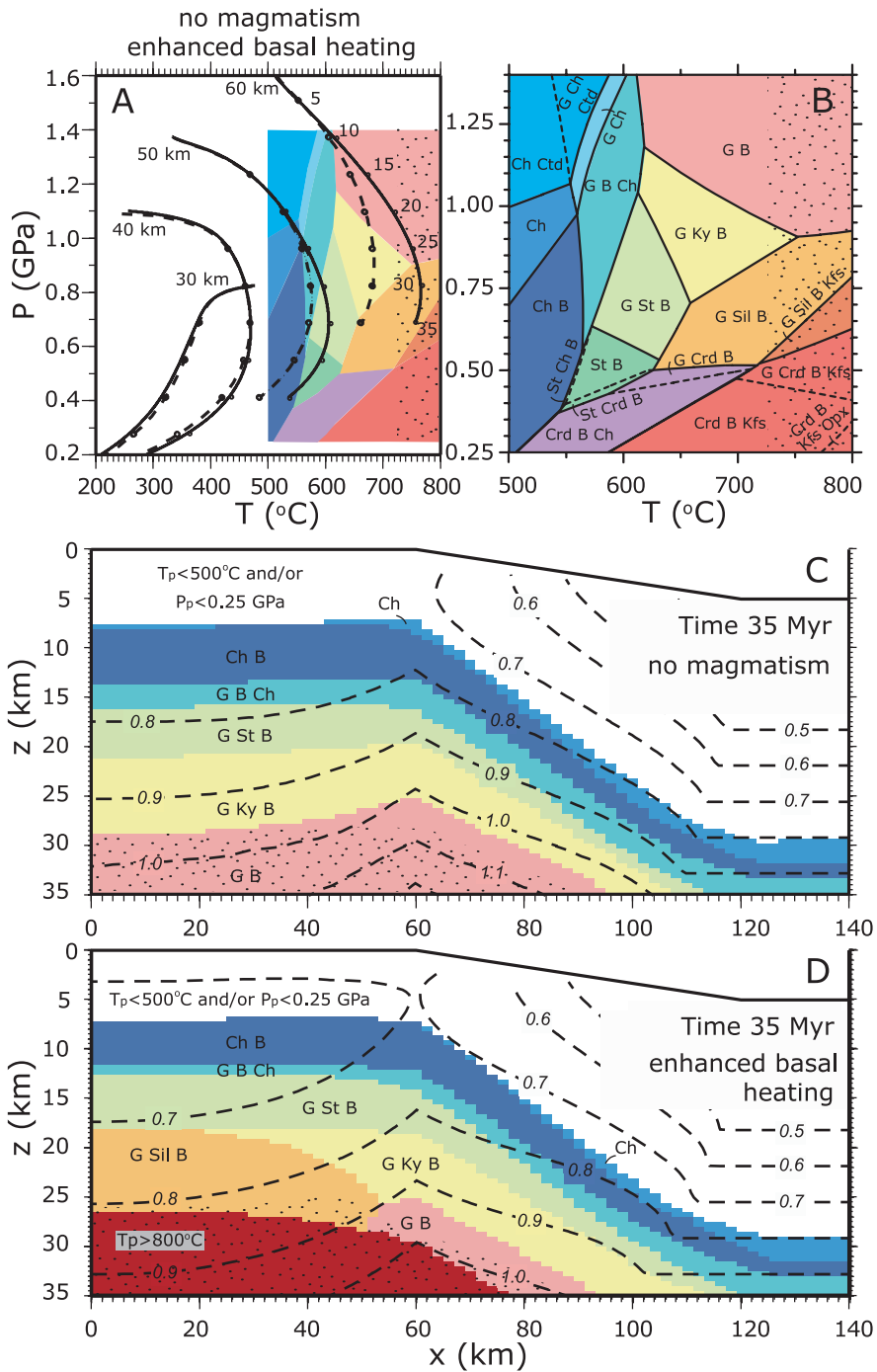


Fig. 9.

assemblages are in the amphibolite facies and include staurolite, kyanite and garnet-biotite (without chlorite). Clearly, this kind of amagmatic model can produce many of the characteristic mineral assemblages found in Barrovian settings. Unlike typical Barrovian metamorphism, however, no peak sillimanite zone mineral assemblages form. The metamorphic field temperature gradients (MFTGs) on the flank of the thrust region are relatively broad; the horizontal transition from the chlorite zone to high-grade mineral assemblages takes place over 20 to 40 km. There are also noticeable pressure changes along the regional MFTGs in some areas reaching 0.3 GPa (fig. 9C). Finally, the model does not produce low-pressure/high-temperature (LP/HT) metamorphism.

The above features observed in a model of regional metamorphism in the absence of additional heat sources and magmas contrast with a number of geologic observations for Dalradian metasediments in the type area of Barrovian and Buchan metamorphism, Scotland (fig. 10). The Grampian orogeny in Scotland lasted c. 10 to 15 Myr and involved significant crustal thickening (to ~70 km) in response to the collision of the Midland Valley Arc with Laurentia beginning ~475 Ma during the closure of the Iapetus Ocean (Dewey, 2005; Oliver and others, 2008). Basin closure is thought to have required considerable northward subduction beneath the Dalradian. Metamorphic pressures in some parts of the Barrovian sequence reached ~1.0 GPa as a result of thickening (Baker, 1985). It is probable that collision was followed by a period (perhaps brief) of thermal relaxation and exhumation of the tectonically-overthickened crust.

The thermal metamorphic peak or peaks that produced the Barrovian and Buchan sequences culminated 465 to 470 Ma (Baxter and others, 2002). Importantly, the regional high-grade amphibolite facies index mineral zones of the Barrovian are evident only in the central and eastern parts of the sequence, and generally formed at pressures of 0.4 to 0.6 GPa (fig. 10). Peak-T conditions for at least three index mineral zones (garnet through kyanite-sillimanite) were attained roughly synchronously (Baxter and others, 2002). The *total* duration of metamorphic mineral growth was considerable. For example, multiple episodes of garnet crystallization spanned ~473 to ~465 Ma (Baxter and others, 2002). However, modeling of elemental diffusion profiles preserved in apatite and garnet demonstrates that the peak thermal pulse (or pulses) was brief; the total integrated timescale was about a million years or less for rocks that reached peak-T conditions at ~0.4 to 0.6 GPa (Ague and Baxter, 2007). There may have been one pulse, or a series of shorter ones spaced out over a longer period of time (Lancaster and others, 2008). This pulsed peak heating at mid-crustal depth is believed to have produced the classic Barrovian index mineral zones and perhaps the lower-P (≤ 0.4 GPa) Buchan sequence to the north as well (fig. 10, Ague and Baxter, 2007).

Fluid flow in the coastal Barrovian sequence north of Stonehaven inferred from petrological data is consistent with flow in a direction of increasing temperature;

Fig. 9. (A) Model P-T-t paths for an overthrust setting with erosion rate 1 mm yr^{-1} in the absence of magmatism. Default model with mantle heat flux equal 35 mW m^{-2} (dashed lines). Model with enhanced mantle heat flux of 70 mW m^{-2} for $x = 1\text{--}60$ km is shown in solid lines. The P-T-t paths are for the rock column located at $x = 10$ km; points mark 5 Myr intervals. Initial rock depth (km) shown for each P-T-t path. (B) Representative pseudosection for aluminous metapelitic rocks in the system $\text{K}_2\text{O}\text{--}\text{FeO}\text{--}\text{MgO}\text{--}\text{Al}_2\text{O}_3\text{--}\text{SiO}_2\text{--}\text{H}_2\text{O}$ (see Part I). For simplicity, partial melting relations are not distinguished graphically, but high-T assemblages ($\geq 725^\circ\text{C}$) are depicted with a stipple pattern on this and subsequent figures. B: biotite; Ch: chlorite; Crd: cordierite; Ctd: chloritoid; G: garnet; Kfs: K-feldspar; Ky: kyanite; Opx: orthopyroxene; Sil: sillimanite; St: staurolite. (C) Peak-T (T_p) metamorphic mineral assemblages at 35 Myr for a model of regional metamorphism with erosion rate 1 mm yr^{-1} after 35 km of exhumation. P_p denotes pressure at peak temperature (GPa). P_p contours shown with dashed lines (GPa). (D) Peak metamorphic assemblages at 35 Myr for a model with enhanced mantle heat flux of 70 mW m^{-2} for $x = 1\text{--}60$ km. P_p contours shown with dashed lines (GPa).

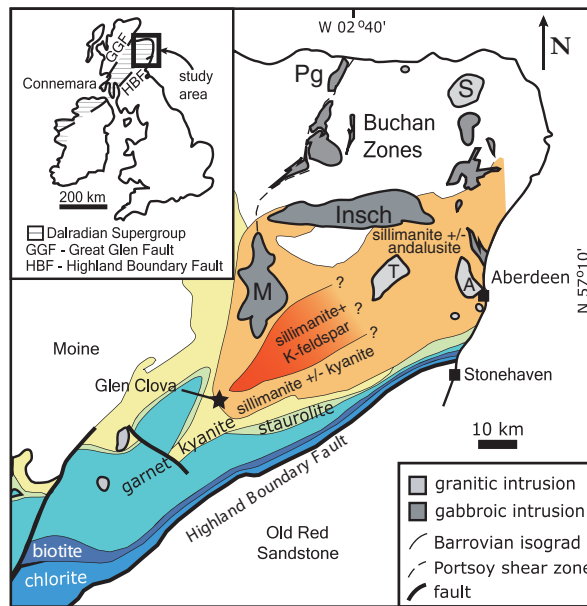


Fig. 10. Sketch map of northeastern Scotland illustrating the Barrovian zones, the region of Buchan metamorphism, and selected Ordovician intrusions. A: Aberdeen Granite; Insch: Insch Gabbro; M: Morven Cabrach Gabbro; Pg: Portsoy Gabbro; S: Strichen Granite; T: Tillyfourie Granite. Modified from Atherton (1977), Baker (1985), Ague and Baxter (2007), Oliver and others (2008), and BGS (2007).

time-integrated fluid flux estimates are on the order of $10^4 \text{ m}^3 \text{ m}^{-2}$ for fracture conduits (Ague, 1997; Masters and Ague, 2005). Exhumation was rapid, and may have locally reached rates of 3 to 7 mm yr^{-1} (Oliver and others, 2000; Oliver and others, 2008).

Several large (more than 10 km across), broadly syn-metamorphic granitic and gabbroic intrusions crop out within the Barrovian and Buchan zones (fig. 10; Gramscian Event granites and Newer Gabbros; compare Oliver and others, 2008). Conspicuous among these is the Insch Gabbro, a large (43 km \times 8 km), layered, sheet-like body that has an exposed thickness of \sim 1 km but which is probably at least 5 km thick (Clarke and Wadsworth, 1970; Leslie, 1984). It, as well as the adjacent Morven Cabrach Gabbro and Portsoy Gabbro, was intruded at or very near the metamorphic peak (c. 470–475 Ma; Dempster and others, 2002; Oliver and others, 2008). The felsic intrusions are two-mica granites inferred to have been sourced, at least in part, from partial melting of metasediments, whereas the mafic intrusions are thought to have been derived from a spinel ilherzolite mantle source (Oliver and others, 2008). Consequently, the gabbros provide clear evidence for the addition of heat and mass from the mantle into the thickened crustal section at the time of regional metamorphism. The MFTGs into the high-grade Barrovian zones along the Highland Boundary Fault nearest the zone of intrusions in the southeastern part of figure 10 are very steep; the transition from chlorite to sillimanite zone takes place over just a few km in some areas. To the southwest, away from major intrusions, the MFTGs are much broader, circumscribing tens of kilometers (fig. 10).

The deformation histories and possible heat sources for the Barrovian and Buchan sequences in Scotland have long been discussed in the literature. For example, some studies suggested that the thermal peak (or peaks) was driven by the syn-orogenic mafic intrusions (for example, Pankhurst, 1974; Ashworth, 1975; Baxter and others,

2002). At least part of the mafic intrusive activity occurred along the Portsoy Shear Zone and, thus, some degree of shear heating could also have been important (Viète and others, 2006). However, the importance of shear heating has to be viewed with caution, as metamorphic devolatilization reactions could have consumed much of the heat unless shear zone activity was intense and protracted (compare Lyubetskaya and Ague, 2009b). Harte and Hudson (1979) inferred that Barrovian field P-T gradients, except adjacent to the Highland Boundary Fault, resulted from widespread magmatism in the deep crust below the present level of exposure. Indeed, Barrow (1893) argued that magmas supplied the heat for the metamorphic sequence that bears his name. In contrast to hypotheses involving direct magma intrusion, Oliver and others (2008) proposed that hot asthenosphere that rose through a lithospheric slab break-off or tear was the heat source for the Barrovian metamorphism. The mechanism for the development of steep MFTGs adjacent to the HBF (southeastern part of fig. 10) is also a subject of debate: these gradients are considered a primary thermal feature by some workers (Dempster and others, 2000) and the result of tectonic deformation by others (Harte and Hudson, 1979; Harte and Dempster, 1987).

Our modeling suggests that pulsed magmatism provides a plausible explanation for the major aspects of regional high-temperature metamorphism in the Scottish Dalradian. Although we do not attempt to specifically reconstruct the evolution of the Barrovian and Buchan zones in Scotland, our models show many features similar to those observed in these localities. In figure 11 we illustrate example model results for mid-crustal mafic magmatism initiated at 15 Myr after the start of exhumation. Obviously, an enormous range of other initial and boundary conditions could be considered; we draw attention to the following general phenomena observed both in the field and in the simulation results.

(1) Short thermal peaks spanning timescales less than 1 Myr (fig. 11A, B; Ague and Baxter, 2007). In contrast, models that lack magmatism predict that rocks will maintain temperatures at or very near peak values for at least 5 to 10 Myr. Moreover, large-scale shear or viscous deformational heating to amphibolite facies/partial melting conditions would also be expected to require c. 10^7 years to develop (Whittington and others, 2009).

(2) Near synchronicity of peak temperature attainment over a range of metamorphic zones and depths (fig. 11A, B; Baxter and others, 2002). Amagmatic models, on the other hand, predict a significant range in the timing and depth of peak temperature attainment (~ 5 Myr for 10 km of depth difference at an erosion rate of 1 mm yr^{-1}).

(3) Steep MFTG in the vicinity of magmatic intrusions and broad MFTG related to crustal overthickening at the flank of the zone of crustal thickening. In particular, note that transitions from lower greenschist to upper amphibolite facies mineral assemblages can take place over as little as a few km at $x \sim 40$ km in figures 11C and 11D. Our modeling indicates that the observed steep MFTG could indeed be a primary thermal feature (see figs. 10 and 11C, D), perhaps modified to some degree by post-metamorphic deformation.

(4) Chemical alteration around fractures along the coastal region north of Stonehaven (fig. 10) that is consistent with up-T fluid flow and large time-integrated fluxes (Ague, 1997; Masters and Ague, 2005). The results of this study suggest that upward flow toward intrusions is a viable way to generate large, up-T fluid fluxes in middle and lower crustal rocks undergoing devolatilization. Syn-metamorphic intrusions are rare or absent to the southwest of the area shown in figure 10 at the present level of exposure. Here, chlorite, biotite, and garnet are the regional metamorphic mineral zones. Much remains to be learned regarding fluid flow regimes relative to temperature gradients in this region. If up-T flow signatures are found in the absence

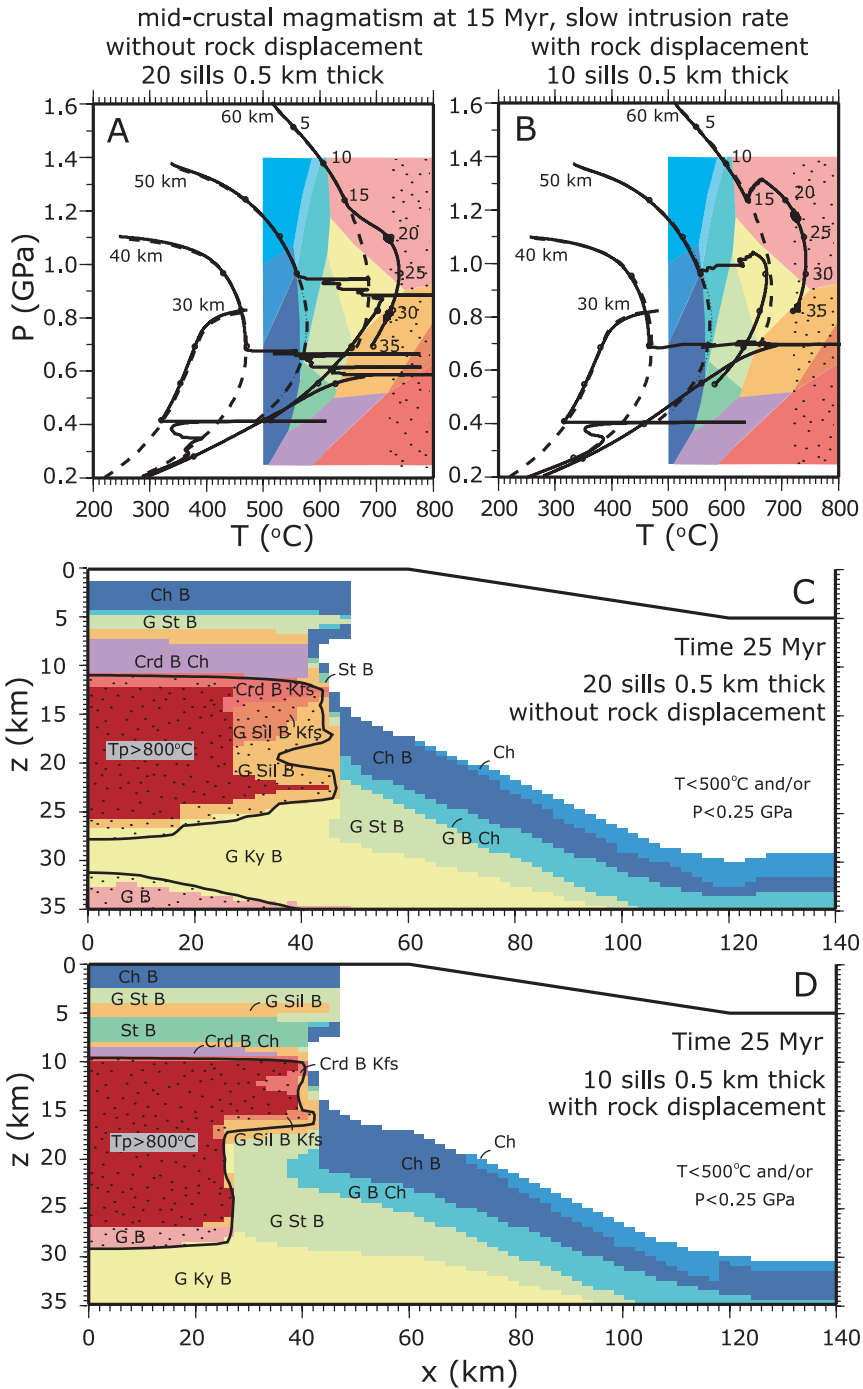


Fig. 11.

of magmatism, it is possible that they developed in response to an inverted geotherm during or immediately following collision (Lyubetskaya and Ague, 2009a). Even in the “type” area shown in figure 10, unraveling the pre-, syn-, and post-magmatic flow regimes is an ongoing challenge.

(5) The broadly penecontemporaneous generation of Barrovian metamorphic sequences at mid–lower crustal depths, and LP/HT (Buchan) sequences at shallower crustal levels (fig. 11; Harte and Hudson, 1979; Oliver and others, 2000). We note that our models predict LP/HT mineral assemblages containing cordierite that are comparable to those found in the Buchan sequence, but do not predict the andalusite-bearing assemblages that are also present. This result is primarily due to the bulk composition used for the pseudosections in our modeling. A slightly more aluminous bulk composition would predict much more widespread andalusite. Similar arguments apply for the kyanite zone. We emphasize that the pseudosection we use is representative, but that a wider spectrum of bulk compositions would have to be investigated to model all possible Barrovian and Buchan mineral assemblages.

(6) The results in figure 11 predict a large area of granulite facies metamorphism. Baker and Droop (1983) and Baker (1985) showed that the heart of the Barrovian sillimanite zone also contains uppermost amphibolite to granulite facies mineral assemblages (fig. 10). Metapelitic rocks contain K-feldspar + sillimanite + garnet + biotite, and metabasalts contain clinopyroxene; peak temperatures were ca. 800 °C (Baker and Droop, 1983; Baker, 1985). The size of the model granulite facies region in figure 11 may be larger than that in the Dalradian, but we emphasize that this result is model dependent such that a smaller volume of magma or lower intrusion temperatures would produce a correspondingly smaller granulite facies region (see fig. 12 in Part I).

(7) A further prediction is that Barrovian metamorphic rocks in the upper greenschist and amphibolite facies would have undergone a relatively high-P early metamorphic history related to overthickening, followed by lower-P (ca. 0.4–0.6 GPa) peak thermal conditions. This prediction remains to be verified or refuted by detailed petrologic analysis, but emerging evidence suggests that this type of P-T path was followed by sillimanite zone rocks at the Barrovian type locality of Glen Clova (Vorhies and Ague, 2009).

Figures 9A and 9D provide useful points of comparison for the scenario of asthenospheric rise into a lithospheric window (Oliver and others, 2008). The P-T-t paths shown with solid lines in figure 9A are for a model of an overthrust setting with an elevated mantle heat flux underneath the thickened crust section at $x = 0$ –60 km. The basal heat flux value of $q_b = 70 \text{ mW m}^{-2}$ is double that of the default model. The peak mineral assemblage distribution for the elevated heat flux case is illustrated in figure 9D. The model is not capable of producing LP/HT metamorphism, as temperatures are not high enough in the shallow crust. Furthermore, the model does not produce steep MFTG or any significant mid-crustal up-T fluid flow. Unlike the classic

Fig. 11. (A) Model P-T-t paths for erosion rate 1 mm yr^{-1} in the absence of magmatism (dashed lines) and for a model with 20 mafic sills 500 m thick intruded every 200 kyr in the depth interval of 15–35 km beginning at 15 Myr without wall rock displacement (solid lines). Temperature fluctuations at $\sim 715 \text{ }^\circ\text{C}$ are related to the initiation or termination of partial melting in metapelitic rocks and result from the relatively sparse numerical grid and the shape of the melting function (see Appendix, Part I). (B) Model P-T-t paths for erosion rate 1 mm yr^{-1} in the absence of magmatism (dashed lines) and for a model with 10 mafic sills 500 m thick intruded every 200 kyr in the depth interval of 15–35 km beginning at 15 Myr with downward vertical wall rock displacement (solid lines). (C) Metamorphic mineral assemblages at 25 Myr for model in part A. Rocks that reached $T \geq 725 \text{ }^\circ\text{C}$ are shown with a stipple pattern bordered by the $725 \text{ }^\circ\text{C}$ contour. These conditions were reached some time prior to or including the model time. Thus the contours and stipple pattern do not represent the T field at 25 Myr. (D) Metamorphic assemblages at 25 Myr for model in part B.

Scottish sequences such as the type Barrovian locality at Glen Clova, the sillimanite-muscovite zone of metamorphism develops at relatively high pressure (0.7-0.9 GPa), because the major heat source is in close proximity to the base of the crust. The peak conditions are not synchronous for rocks at different depths and the timescales of peak-T attainment exceed 5 Myr. Even at higher values of basal heat ($q_b = 90 \text{ mW m}^{-2}$, not shown) the model P-T-t paths have broad asynchronous peaks and LP/HT metamorphism does not develop.

The temperature-time paths for the model with enhanced basal heating and for three different models with mid-crustal (15-35 km depth) magmatism are compared in figure 12. Clearly, a model of enhanced mantle heat flux (fig. 12A) does not produce a strong, narrow thermal peak (or peaks) in the T-t paths. On the other hand, all models with mid-crustal magmatism, despite some differences in the amount of magmatism and intrusion rates (fig. 12B-D), result in T-t paths that contain transient thermal behavior. Transient thermal behavior is compatible with peak Barrovian metamorphism in and around the Glen Clova type locality (Ague and Baxter, 2007). This suggests that Barrovian and perhaps Buchan metamorphism in Scotland were produced by pulsed magmatic heating, although the initiation of magmatism may have been triggered by the kind of asthenospheric upwelling discussed by Oliver and others (2008).

Exhumation rates for the Grampian after the peak of metamorphism may have been larger, at least transiently, than those used in the foregoing models (compare Oliver and others, 2000, 2008). However, very rapid exhumation, in and of itself, is unable to account for major features of the prograde metamorphism across the region. All of the issues evident for metamorphism in the absence of additional crustal heat sources remain. In figure 13 we show results for an exhumation rate of 5 mm yr^{-1} , both the default and a strongly enhanced mantle heat flux, and no magmatism. The peak temperatures are much lower than for slower exhumation, as radiogenic heating does not have as long to operate. Although this type of model does not solve the problems of Barrovian and Buchan metamorphism in and around the type locality, it could be relevant farther to the southwest of the region shown in figure 10 where, at least at the present level of exposure, syn-metamorphic intrusions are rare or absent. There, metamorphic grade only reached the chlorite, biotite, or garnet zones; rapid exhumation at some point following crustal overthickening may have acted to keep metamorphic temperatures relatively low.

On balance, we conclude that the available data are most consistent with the hypothesis that the peak thermal conditions of Barrovian, and probably Buchan, metamorphism were driven by syn-metamorphic magmatism during or following collision. It is likely that the mafic magmas (Newer Gabbros) were the primary cause; their heat could also have been important for partial melting of the metasedimentary source components necessary for the genesis of the two-mica granites. In addition, the rise of asthenosphere (Oliver and others, 2008) may have been an important metamorphic heat source at the deeper crustal levels. Moreover, this rise could have triggered the generation of the mafic partial melts that intruded the metamorphic belt. Considerable uncertainty regarding magma petrogenesis persists, however, and other processes, such as the generation of mafic arc magmas above a subduction zone, must also be investigated.

Oliver and others (2008) point out that the hot zone model of mafic magma intrusion and associated crustal interaction (Annen and Sparks, 2002; Annen and others, 2006) would be expected to produce "I-type" magmas, but large, Grampian-age, I-type intrusions are absent from the Scottish Dalradian. There are several possible reasons for this apparent discrepancy. (1) It is possible that the mafic magmas intruded only into mid-crustal levels such that ambient conditions were not hot enough for the

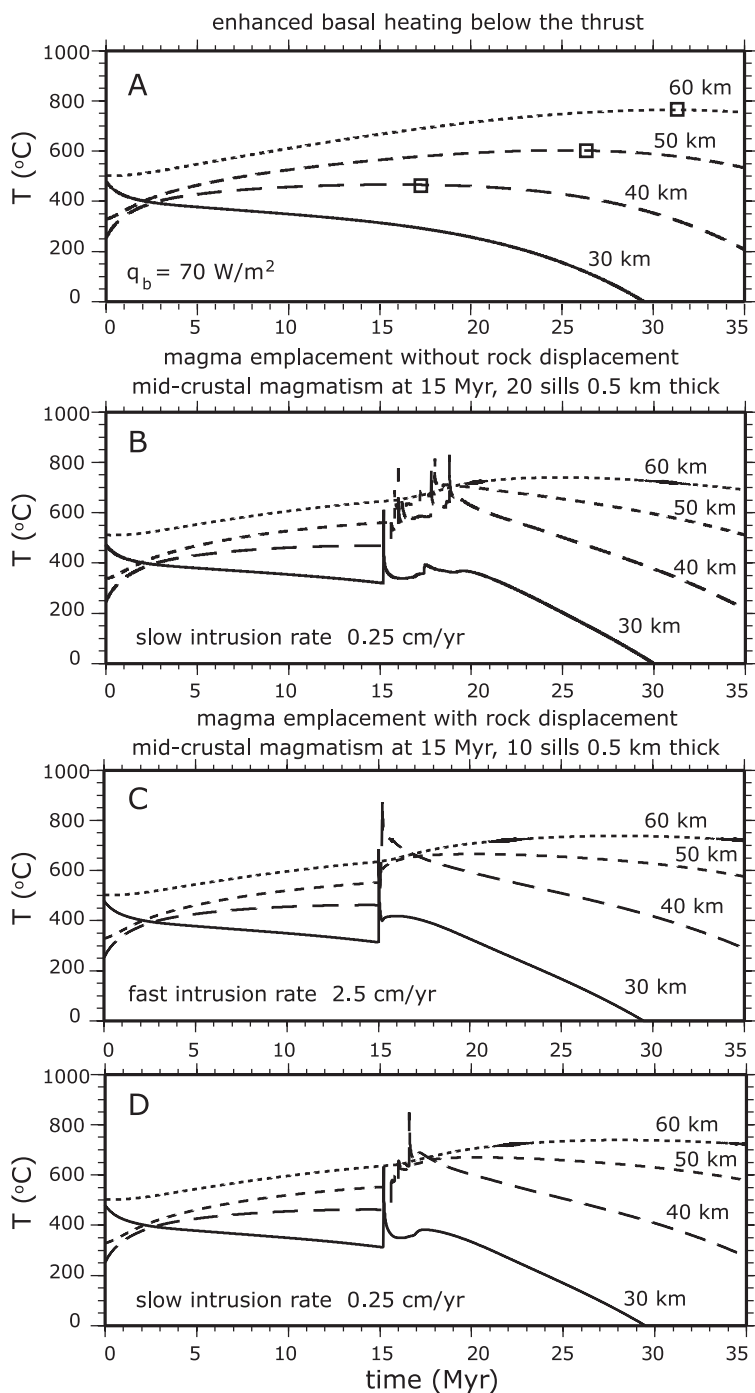


Fig. 12. Temperature-time paths for rocks initially at 30, 40, 50 and 60 km depth and $x = 10$ km. (A) Model with enhanced mantle heat flux of 70 mW m^{-2} for $x = 1-60$ km (see fig. 9A, D). Squares mark the peak temperature conditions. Note that the timing of peak T attainment varies by ~ 15 Myr depending on depth. (B) Model with 20 mafic sills 500 m thick intruded every 200 kyr in the depth interval of 15–35 km beginning at 15 Myr without wall rock displacement. (C) Model with 10 mafic sills 500 m thick intruded every 20 kyr in the depth interval of 15–35 km beginning at 15 Myr with downward vertical wall rock displacement. (D) Same as C but with sills intruded every 200 kyr.

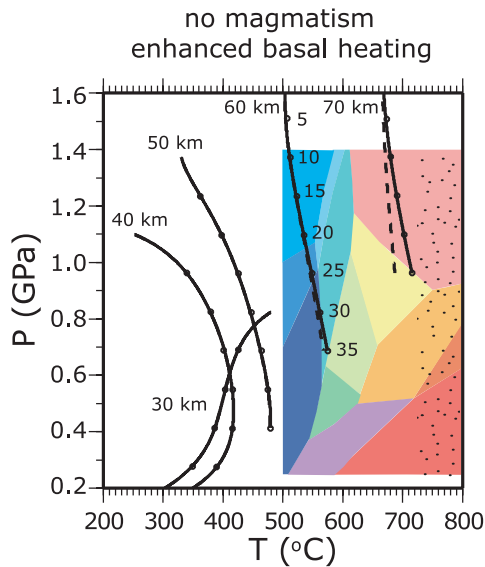


Fig. 13. Model P-T-t paths for erosion rate 5 mm yr^{-1} , in the absence of magmatism. Default model with mantle heat flux of 35 mW m^{-2} (dashed lines). Model with strongly enhanced mantle heat flux of 105 mW m^{-2} for $x = 1\text{--}60 \text{ km}$ is shown in solid lines. The P-T-t paths are for the rock column located at $x = 10 \text{ km}$; points mark 5 Myr intervals.

widespread genesis of I-types (Oliver and others, 2008; see fig. 8A with low fraction of partial melt in mid-crustal magmatism models). (2) If the I-type magmas had relatively low water contents, they could have ascended through the metamorphic sequence to shallow crustal levels before crystallizing. In this scenario, they would have been removed by erosion and, thus, absent from the field area today. (3) It is also possible that melts of broadly I-type composition remained more or less *in situ*; we note that pre-existing metamorphic rocks in the highest-grade parts of the Barrovian underwent widespread migmatization and the formation of quartz + plagioclase \pm hornblende \pm biotite leucosomes (Baker and Droop, 1983). (4) Finally, and perhaps most significantly, the hot zone model presented by Annen and others (2006) was focused on the production of large volumes of intermediate and silicic magmas in arcs. In these environments, massive amounts of mafic magma must be emplaced to supply the necessary heat and mass required for major partial melting of the crust (total thickness of sills $> 15 \text{ km}$). Our work considers more modest sill volumes (default total thickness = 5 km) in order to supply significant heat without causing large-scale arc magma genesis. In Scotland, it is possible that the amount of mafic magma input was sufficient to cause metamorphic thermal pulses, but not extensive enough to cause full-scale arc magmatism. More specific modeling attuned to the finer details of magmatic-metamorphic interactions is necessary to obtain a better understanding of the heat sources for Barrovian- and Buchan-type metamorphism in Scotland and in mountain belts worldwide.

CONCLUDING REMARKS

The models make a number of testable predictions about post-collisional P-T-t evolution in orogens intruded by magmas. One overarching prediction that has also been discussed by previous workers is that regional metamorphic temperatures in magmatic settings can be much greater than those attainable by simple thermal

relaxation of overthickened crust. This will be particularly noticeable for magma intrusion at intermediate-shallow crustal levels, which can produce the elevated thermal gradients necessary for widespread amphibolite facies metamorphism at pressures less than about 0.6 GPa. Steep metamorphic field temperature gradients are predicted on the flanks of the magmatic zones (figs. 10, 11).

The specific metamorphic regimes that develop depend on a host of geologic factors, including magma emplacement T , wall rock T , volume of magma, and depth. Buchan, Barrovian, and granulite facies metamorphism can all develop penecontemporaneously in relatively close proximity during mid-crustal magmatism (fig. 11). The effects of deep-crustal magmatism may be difficult to distinguish from those of elevated mantle heat flow, particularly if the mafic crustal root delaminates and is not preserved. However, regardless of the depth of intrusion, the models predict that fluid flow in a direction of increasing temperature will occur beneath and on the flanks of intrusions, particularly if magmatism takes place relatively early in the exhumation history (fig. 2). If fluxes are large enough, this flow can produce a number of identifiable phenomena in metamorphic rocks, including chemical metasomatism, such as the bulk-rock exchange of Na for K (Masters and Ague, 2005); infiltration-driven devolatilization reactions in metacarbonate rocks that release CO_2 (Ferry, 1992); and systematic shifts in stable isotope (O, H) ratios (Dipple and Ferry, 1992). Widespread hydrofracturing (fig. 6) and isotopic signatures indicative of fluid-rock interactions involving fluids derived from (or equilibrated with) intrusions would also be expected.

The pace of magma intrusion will largely control the rates of heating and, thus, the timing of peak thermal events and associated devolatilization. Consequently, radiometric dating will reveal close temporal links between magmatic activity and metamorphic episodes. If intrusion occurs over a geologically short time interval, then the magma-driven thermal pulse or pulses will result in peak metamorphism that is roughly synchronous over a range of crustal depths. Because heat transfer away from the intrusions will be largely controlled by conduction through the rock mass, the pulse or pulses will be most temporally distinct proximal to intrusions, and be more diffuse farther away. Consequently, P-T-t paths for wall rocks proximal to magmatism will be characterized by approximately isobaric thermal transients, whereas thermal responses will be much broader in distal rocks (compare rocks initially at 40 km and 60 km depths, fig. 11A, B). In addition, for mid-crustal magmatism, the broad thermal peaks for the deepest rocks outside the zone of magmatism will lag those in or near the zone of magmatism by 5 to 15 Ma (fig. 12B-D). The timing will, of course, be different for different erosion rates.

On the other hand, if intrusive activity is spaced out over wide time intervals during exhumation, then peak thermal conditions need not be penecontemporaneous spatially or across metamorphic grades. Nonetheless, the timing relations as functions of depth and grade could be very different than for the case of post-collisional amagmatic thermal relaxation of overthickened crust. The relaxation model predicts that the youngest metamorphic ages will be found in the highest-grade, most deeply-exhumed rocks, and the oldest ages in the shallowest (England and Thompson, 1984). In contrast, if magmatism is an important driver for metamorphism, then the highest-grade peak-T conditions need not be restricted to the most deeply-exhumed rocks (figs. 11, 12). Instead, the depths at which peak conditions are attained will correspond to the crustal levels of magma emplacement. Regardless of the pace of magmatism—whether condensed or spread out in time—the input of magmatic heat will cause P-T-t paths to depart from the simple clockwise evolution predicted by the relaxation model; these departures to higher temperatures can be resolved by modern thermobarometry, geochronology, and pseudosection analysis.

Rapid input of heat from magmas will produce pulsed growth of metamorphic minerals that can be recorded by chemical and isotopic zoning in refractory minerals such as garnet. Pseudosection analysis can identify the growth histories that produced the mineral zoning and mineral assemblages, thus constraining P-T paths (Powell and Holland, 2008). Furthermore, modeling the partial diffusive relaxation of growth zoning in metamorphic minerals can provide critical constraints on the timescales of thermal activity (for example, Faryad and Chakraborty, 2005; Ague and Baxter, 2007). Importantly, magma-driven thermal pulses will produce changes in the rates of heating and mineral growth; these rate changes can now be resolved with high-precision/high-spatial resolution isotopic dating of porphyroblasts (Sm/Nd garnet-whole rock dating; Pollington and Baxter, 2010). This kind of geochronology can determine the absolute timing of multiple growth pulses during the crystallization of single crystals and, therefore, whether or not regional thermal anomalies were caused by one intrusive episode, or multiple episodes.

Regional mafic magma intrusion will in general require significant mass (and thus heat) input from the mantle. Consequently, syn-metamorphic intrusions should carry the trace element and isotopic signatures of mantle source components (unless the intrusions are completely derived from crustal partial melting). If the magmatic flux from the mantle is very large, then arc-type magmatism along the lines of the hot zone model will develop (Annen and others, 2006). In such cases, large-scale generation and ascent of intermediate and silica melts may obliterate metamorphic zones formed earlier in the intrusion history.

ACKNOWLEDGMENTS

We thank E. F. Baxter, D. Bercovici, D. M. Rye, and R. S. J. Sparks for their insights regarding fluid and heat flow, and S. C. Penniston-Dorland and J. A. D. Connolly for their critical reviews which greatly improved this paper. The support of the National Science Foundation Directorate for Geosciences (NSF EAR-0509934) is gratefully acknowledged.

REFERENCES

- Ague, J. J., 1994, Mass transfer during Barrovian metamorphism of pelites, south-central Connecticut: II. Channelized fluid flow and the growth of staurolite and kyanite: *American Journal of Science*, v. 294, p. 1061–1134.
- 1997, Crustal mass transfer and index mineral growth in Barrow's garnet zone, northeast Scotland: *Geology*, v. 25, p. 73–76, doi: 10.1130/0091-7613(1997)025<0073:CMTAIM>2.3.CO;2.
- 2000, Release of CO₂ from carbonate rocks during regional metamorphism of lithologically heterogeneous crust: *Geology*, v. 28, p. 1123–1126, doi: 10.1130/0091-7613(2000)28<1123:ROCFCR>2.0.CO;2.
- Ague, J. J., and Baxter, E. F., 2007, Brief thermal pulses during mountain building recorded by Sr diffusion in apatite and multicomponent diffusion in garnet: *Earth and Planetary Science Letters*, v. 261, p. 500–516, doi: 10.1016/j.epsl.2007.07.017.
- Ague, J. J., and Rye, D. M., 1999, Simple models of CO₂ release from metacarbonates with implications for interpretation of directions and magnitudes of fluid flow in the deep crust: *Journal of Petrology*, v. 40, p. 1443–1462, doi: 10.1093/petroj/40.9.1443.
- Ague, J. J., Park, J., and Rye, D. M., 1998, Regional metamorphic dehydration and seismic hazard: *Geophysical Research Letters*, v. 25, p. 4221–4224, doi: 10.1029/1998GL900124.
- Annen, C., and Sparks, R. S. J., 2002, Effects of repetitive emplacement of basaltic intrusions on thermal evolution and melt generation in the crust: *Earth and Planetary Science Letters*, v. 203, p. 937–955, doi: 10.1016/S0012-821X(02)00929-9.
- Annen, C., Blundy, J. D., and Sparks, R. S. J., 2006, The genesis of intermediate and silicic magmas in deep crustal hot zones: *Journal of Petrology*, v. 47, p. 505–539, doi: 10.1093/petrology/egi084.
- Ashworth, J. R., 1975, The sillimanite zones of the Huntly-Portsoy area in the north-eastern Dalradian, Scotland: *Geological Magazine*, v. 112, p. 113–224, doi: 10.1017/S0016756800045817.
- Atherton, M. P., 1977, The metamorphism of the Dalradian rocks of Scotland: *Scottish Journal of Geology*, v. 13, p. 331–370, doi: 10.1144/sjg13040331.
- Baker, A. J., 1985, Pressures and temperatures of metamorphism in the Eastern Dalradian: *Journal of the Geologic Society, London*, v. 142(1), p. 137–148, doi: 10.1144/gsjgs.142.1.0137.
- Baker, A. J., and Droop, G. T. R., 1983, Grampian metamorphic conditions deduced from mafic granulites

- and sillimanite-K-feldspar gneisses in the Dalradian of Glen Muick, Scotland: *Journal of the Geological Society, London*, v. 140, p. 489–498, doi: 10.1144/gsjgs.140.3.0489.
- Balashov, V. N., and Yardley, B. W. D., 1998, Modeling metamorphic fluid flow with reaction-compaction-permeability feedbacks: *American Journal of Science*, v. 298, p. 441–470.
- Barrow, G., 1893, On an intrusion of muscovite-biotite gneiss in the south-east Highlands of Scotland and its accompanying metamorphism: *Geological Society of London Quarterly Journal*, v. 49, p. 330–358, doi: 10.1144/GSL.JGS.1893.049.01-04.52.
- Baumgartner, L. P., and Ferry, J. M., 1991, A model for coupled fluid-flow and mixed-volatile mineral reactions with applications to regional metamorphism: *Contributions to Mineralogy and Petrology*, v. 106, p. 273–285, doi: 10.1007/BF00324557.
- Baxter, E. F., Ague, J. J., and DePaolo, D. J., 2002, Prograde temperature-time evolution in the Barrovian type-locality constrained by Sm/Nd garnet ages from Glen Clova, Scotland: *Journal of the Geological Society, London*, v. 159, p. 71–82, doi: 10.1144/0016-76901013.
- Bickle, M. J., and Baker, J., 1990, Advective-diffusive transport of isotopic fronts: an example from Naxos, Greece: *Earth and Planetary Science Letters*, v. 97, p. 79–93, doi: 10.1016/0012-821X(90)90100-C.
- British Geological Survey, 2007, *Bedrock Geology UK North (small scale geology maps)*, 5th edition: British Geological Survey, Keyworth, Nottingham, scale 1:625,000.
- Burg, J.-P., and Gerya, T. V., 2005, The role of viscous heating in Barrovian metamorphism of collisional orogens: thermomechanical models and application to the Lepontine Dome in the Central Alps: *Journal of Metamorphic Geology*, v. 23, p. 75–95, doi: 10.1111/j.1525-1314.2005.00563.x.
- Chamberlain, C. P., and Rumble, D., III, 1989, The influence of fluids on the thermal history of a metamorphic terrain: New Hampshire, USA, in Daly, J. S., Cliff, R. A., and Yardley, B. W. D., editors, *Evolution of Metamorphic Belts*: Geological Society, London, Special Publications, v. 43, p. 203–213, doi: 10.1144/GSL.SP.1989.043.01.13.
- Clarke, P. D., and Wadsworth, W. J., 1970, The Insh layered intrusion: *Scottish Journal of Geology*, v. 6, p. 7–25, doi: 10.1144/sig06010007.
- Connolly, J. A. D., 1997, Devolatilization-generated fluid pressure and deformation-propagated fluid flow during prograde regional metamorphism: *Journal of Geophysical Research*, v. 102, p. 18149–18173, doi: 10.1029/97JB00731.
- 2010, The mechanics of metamorphic fluid expulsion: *Elements*, v. 6, p. 165–172, doi: 10.2113/gselements.6.3.165.
- Connolly, J. A. D., and Podladchikov, Y. Y., 2004, Fluid flow in compressive tectonic settings: Implications for midcrustal seismic reflectors and downward fluid migration: *Journal of Geophysical Research*, v. 109, B04201, doi:10.1029/2003JB002822.
- Connolly, J. A. D., and Thompson, A. B., 1989, Fluid and enthalpy production during regional metamorphism: *Contributions to Mineralogy and Petrology*, v. 102, p. 347–366, doi: 10.1007/BF00373728.
- Dempster, T. J., Fallick, A. E., and Whitemore, C. J., 2000, Metamorphic reactions in the biotite zone, eastern Scotland: high thermal gradients, metasomatism and cleavage formation: *Contributions to Mineralogy and Petrology*, v. 138, p. 348–363, doi: 10.1007/s004100050568.
- Dempster, T. J., Rogers, G., Tanner, P. W. G., Bluck, B. J., Muir, R. J., Redwood, S. D., Ireland, T. R., and Paterson, B. A., 2002, Timing of deposition, orogenesis and glaciation within the Dalradian rocks of Scotland: constraints from U-Pb ages zircon ages: *Journal of the Geological Society, London*, v. 159, p. 83–94, doi: 10.1144/0016-764901061.
- DePaolo, D. J., 1981, Trace element and isotopic effects of combined wallrock assimilation and fractional crystallization: *Earth and Planetary Science Letters*, v. 53, p. 189–202, doi:10.1016/0012-821X(81)90153-9.
- Dewey, J. F., 2005, Orogeny can be very short: *Proceedings of the National Academy of Sciences*, v. 102, p. 15286–15293, doi: 10.1073/pnas.0505516102.
- Dipple, G. M., and Ferry, J. M., 1992, Fluid flow and stable isotopic alteration in rocks at elevated temperatures with applications to metamorphism: *Geochimica et Cosmochimica Acta*, v. 56, p. 3539–3550, doi: 10.1016/0016-7037(92)90397-2.
- England, P. C., and Thompson, A. B., 1984, Pressure-Temperature-Time paths of regional metamorphism. I. Heat transfer during the evolution of regions of thickened continental crust: *Journal of Petrology*, v. 25, p. 894–928, doi: 10.1093/petrology/25.4.894.
- Etheridge, M. A., Wall, V. J., Cox, S. F., and Vernon, R. H., 1984, High fluid pressures during regional metamorphism and deformation: Implications for mass transport and deformation mechanisms: *Journal of Geophysical Research*, v. 89, p. 4344–4358, doi: 10.1029/JB089iB06p04344.
- Evans, K. A., and Bickle, M. J., 1999, Determination of time-integrated metamorphic fluid fluxes from the reaction progress of multivariant assemblages: *Contributions to Mineralogy and Petrology*, v. 134, p. 277–293, doi: 10.1007/s004100050484.
- Faryad, S. W., and Chakraborty, S., 2005, Duration of Eo-Alpine metamorphic events obtained from multicomponent diffusion modeling of garnet: a case study from the Eastern Alps: *Contributions to Mineralogy and Petrology*, v. 150, p. 306–318, doi: 10.1007/s00410-005-0020-0.
- Ferry, J. M., 1992, Regional metamorphism of the Waits River Formation, eastern Vermont: delineation of a new type of giant metamorphic hydrothermal system: *Journal of Petrology*, v. 33, p. 45–94, doi: 10.1093/petrology/33.1.45.
- Flekkøy, E. G., Malthe-Sørenssen, A., and Jamtveit, B., 2002, Modeling hydrofracture: *Journal of Geophysical Research*, v. 107, article n. 2151, doi:10.1029/2000JB000132.
- Garven, G., and Freeze, R. A., 1984, Theoretical analysis of the role of groundwater flow in the genesis of stratabound ore deposits: 2. Quantitative results: *American Journal of Science*, v. 284, p. 1125–1174.
- Haack, U. K., and Zimmermann, H. D., 1996, Retrograde mineral reactions: a heat source in the continental crust?: *Geologische Rundschau*, v. 85, p. 130–137, doi: 10.1007/BF00192071.

- Hanson, R. B., 1997, Hydrodynamics of regional metamorphism due to continental collision: *Economic Geology*, v. 92, p. 880–891, doi: 10.2113/gsecongeo.92.7-8.880.
- Harte, B., and Dempster, T. J., 1987, Regional metamorphic zones: tectonic controls: *Philosophical Transactions of the Royal Society of London*, v. A321, p. 105–127.
- Harte, B., and Hudson, N. F. C., 1979, Pelite facies series and the temperatures and pressures of Dalradian metamorphism in E Scotland, *in* Harris, A. L., Holland, C. H., and Leake, B. E., editors, *The Caledonides of the British Isles—Reviewed*: Geological Society, London, Special Publications, v. 8, p. 323–337, doi: 10.1144/GSL.SP.1979.008.01.36.
- Hiraga, T., Nishikawa, O., Nagase, T., and Akizuki, M., 2001, Morphology of intergranular pores and wetting angles in pelitic schists studied by transmission electron microscopy: *Contributions to Mineralogy and Petrology*, v. 141, p. 613–622, doi: 10.1007/s004100100263.
- Horne, J., 1884, The origin of the andalusite-schists of Aberdeenshire: *Mineralogical Magazine*, v. 6, p. 98–100, doi: 10.1180/minmag.1884.006.028.06.
- Huerta, A. D., Royden, L. H., and Hodges, K. V., 1996, The interdependence of deformational and thermal processes in mountain belts: *Science*, v. 273, p. 637–639, doi: 10.1126/science.273.5275.637.
- Ingebritsen, S. E., and Manning, C. E., 2010, Permeability of the continental crust: dynamic variations inferred from seismicity and metamorphism: *Geofluids*, v. 10, p. 193–205, doi: 10.1111/j.1468-8123.2010.00278.x.
- Iyer, K., Jamtveit, B., Mathiesen, J., Malthe-Sørensen, A., and Feder, J., 2008, Reaction-assisted hierarchical fracturing during serpentinization: *Earth and Planetary Science Letters*, v. 267, p. 503–516, doi:10.1016/j.epsl.2007.11.060.
- Jamieson, R. A., Beaumont, C., Fullsack, P., and Lee, B., 1998, Barrovian regional metamorphism: where's the heat? *in* Treolar, P. J., and O'Brien, P. J., editors, *What Drives Metamorphism and Metamorphic Reactions?*: Geological Society, London, Special Publications, v. 138, p. 23–51, doi: 10.1144/GSL.SP.1996.138.01.03.
- Koons, P. O., and Craw, D., 1991, Evolution of fluid driving forces and composition within collisional orogens: *Geophysical Research Letters*, v. 18, p. 935–938, doi: 10.1029/91GL00910.
- Lancaster, P. J., Baxter, E. F., Ague, J. J., Breeding, C. M., and Owens, T. L., 2008, Synchronous peak Barrovian metamorphism driven by syn-orogenic magmatism and fluid flow in southern Connecticut, USA: *Journal of Metamorphic Geology*, v. 26, p. 527–538, doi: 10.1111/j.1525-1314.2008.00773.x.
- Leslie, A. G., 1984, Field relations in the north-eastern part of the Insh mafic igneous mass, Aberdeenshire: *Scottish Journal of Geology*, v. 20, p. 215–235, doi: 10.1144/sjg20020215.
- Luttge, A., Bolton, E. W., and Rye, D. M., 2004, A kinetic model of metamorphism: an application to siliceous Dolomites: *Contributions to Mineralogy and Petrology*, v. 146, p. 546–565, doi: 10.1007/s00410-003-0520-8.
- Lyubetskaya, T., and Ague, J. J., 2009a, Modeling the magnitudes and directions of regional metamorphic fluid flow in collisional orogens: *Journal of Petrology*, v. 50, p. 1505–1531, doi: 10.1093/petrology/egp039.
- 2009b, Effect of metamorphic reactions on thermal evolution in collisional orogens: *Journal of Metamorphic Geology*, v. 27, p. 579–600, doi: 10.1111/j.1525-1314.2009.00847.x.
- Manning, C. E., and Ingebritsen, S. E., 1999, Permeability of the continental crust: implications of geothermal data and metamorphic systems: *Reviews of Geophysics*, v. 37, p. 127–150, doi: 10.1029/1998RG900002.
- Masters, R. L., and Ague, J. J., 2005, Regional-scale fluid flow and element mobility in Barrow's metamorphic zones, Stonehaven, Scotland: *Contributions to Mineralogy and Petrology*, v. 150, p. 1–18, doi: 10.1007/s00410-005-0005-z.
- Miller, S. A., van der Zee, W., Olgaard, D. L., and Connolly, J. A. D., 2003, A fluid-pressure feedback model of dehydration reactions: experiments, modelling, and application to subduction zones: *Tectonophysics*, v. 370, p. 241–251, doi: 10.1016/S0040-1951(03)00189-6.
- Oliver, G. J. H., Chen, F., Buchwaldt, R., and Hegner, E., 2000, Fast tectonometamorphism and exhumation in the type area of the Barrovian and Buchan zones: *Geology*, v. 28, p. 459–462, doi: 10.1130/0091-7613(2000)28<459:FTAET>2.0.CO;2.
- Oliver, G. J. H., Wilde, S. A., and Wan, Y., 2008, Geochronology and geodynamics of Scottish granitoids from the late Neoproterozoic break-up of Rodinia to Palaeozoic collision: *Journal of the Geological Society*, London, v. 165, p. 661–674, doi: 10.1144/0016-76492007-105.
- Oliver, N. H. S., Dipple, G. M., Cartwright, I., and Schiller, J., 1998, Fluid flow and metasomatism in the genesis of the amphibolite-facies, pelite-hosted Kanmantoo copper deposit, South Australia: *American Journal of Science*, v. 298, p. 181–218.
- Pankhurst, R. J., 1970, The geochronology of the basic igneous complexes: *Scottish Journal of Geology*, v. 6, p. 83–107, doi: 10.1144/sjg06010083.
- 1974, Rb-Sr whole-rock chronology of Caledonian events in north-east Scotland: *Geological Society of America Bulletin*, v. 85, p. 345–350, doi: 10.1130/0016-7606(1974)85<345:RWCOCE>2.0.CO;2.
- Peacock, S. M., 1989, Numerical constraints on rates of metamorphism, fluid production, and fluid flux during regional metamorphism: *Geological Society of America Bulletin*, v. 101, p. 476–485, doi: 10.1130/0016-7606(1989)101<0476:NCOROM>2.3.CO;2.
- Penniston-Dorland, S. C., and Ferry, J. M., 2008, Element mobility and scale of mass transport in the formation of quartz veins during regional metamorphism of the Waits River Formation, east-central Vermont: *American Mineralogist*, v. 93, p. 7–21, doi: 10.2138/am.2008.2461.
- Pollington, A. D., and Baxter, E. F., 2010, High resolution Sm–Nd garnet geochronology reveals the uneven pace of tectonometamorphic processes: *Earth and Planetary Science Letters*, v. 293, p. 63–71, doi: 10.1016/j.epsl.2010.02.019.

- Powell, R., and Holland, T. J. B., 2008, On thermobarometry: *Journal of Metamorphic Geology*, v. 26, p. 155–179, doi: 10.1111/j.1525-1314.2007.00756.x.
- Powell, R., Holland, T., and Worley, B., 1998, Calculating phase diagrams involving solid solutions via non-linear equations, with examples using THERMOCALC: *Journal of Metamorphic Geology*, v. 16, p. 577–588, doi: 10.1111/j.1525-1314.1998.00157.x.
- Ridley, J., 1986, Modelling of the relations between reaction enthalpy and the buffering of reaction progress in metamorphism: *Mineralogical Magazine*, v. 50, p. 375–384, doi: 10.1180/minmag.1986.050.357.03.
- Sleep, N. H., and Blanpied, M. L., 1992, Creep, compaction and the weak rheology of major faults: *Nature*, v. 259, p. 687–692, doi: 10.1038/359687a0.
- Stober, I., and Bucher, K., 2004, Fluid sinks within the earth's crust: *Geofluids* v. 4, p. 143–151, doi: 10.1111/j.1468-8115.2004.00078.x.
- Tenthorey, E., and Cox, S. F., 2003, Reaction-enhanced permeability during serpentinite dehydration: *Geology*, v. 31, p. 921–924, doi: 10.1130/G19724.1.
- van Haren, J. L. M., Ague, J. J., and Rye, D. M., 1996, Oxygen isotope record of fluid infiltration and mass transfer during regional metamorphism of pelitic schist, Connecticut, USA: *Geochimica et Cosmochimica Acta*, v. 60, p. 3487–3504, doi: 10.1016/0016-7037(96)00182-2.
- Viete, D. R., Richards, S. W., and Lister, G. S., 2006, Time-scales and heat sources for Barrovian regional metamorphism, Goldschmidt Conference, 16th, Melbourne, Australia: *Geochimica et Cosmochimica Acta*, v. 70, issue 18, p. A672–A672, doi: 10.1016/j.gca.2006.06.1256.
- Vorhies, S., and Ague, J. J., 2009, Pressure-temperature conditions and pressure-temperature-time paths, Barrovian metamorphic zones, Scotland: *Geological Society of America Abstracts with Programs*, v. 41, n. 7, p. 484.
- Walder, J., and Nur, A., 1984, Porosity reduction and crustal pore pressure development: *Journal of Geophysical Research*, v. 89, n. B13, p. 11539–11548, doi: 10.1029/JB089iB13p11539.
- Walther, J. V., and Orville, P. M., 1984, Volatile production and transport during metamorphism: *Contributions to Mineralogy and Petrology*, v. 79, p. 252–257, doi: 10.1007/BF00371516.
- Whittington, A. G., Hofmeister, A. M., and Nabelek, P. I., 2009, Temperature-dependent thermal diffusivity of the Earth's crust and implications for magmatism: *Nature*, v. 458, p. 319–321, doi: 10.1038/nature07818.
- Wing, B. A., and Ferry, J. M., 2002, Three-dimensional geometry of metamorphic fluid flow during Barrovian regional metamorphism from an inversion of combined petrologic and stable isotope data: *Geology*, v. 30, p. 639–642, doi: 10.1130/0091-7613(2002)030<0639:TDOGMF>2.0.CO;2.
- 2007, Magnitude and geometry of reactive fluid flow from direct inversion of spatial patterns of geochemical alteration: *American Journal of Science*, v. 307, p. 793–832, doi: 10.2475/05.2007.02.
- Yakovlev, L. Ye., 1993, The role of metamorphism of the basaltic basement of sedimentary basins in crustal evolution: *International Geology Review*, v. 35, p. 27–47, doi: 10.1080/00206819309465512.
- Yardley, B. W. D., 2009, The role of water in the evolution of the continental crust: *Journal of the Geological Society, London*, v. 166, p. 585–600, doi: 10.1144/0016-76492008-101.
- Zhang, S., FitzGerald, J. D., and Cox, S. F., 2000, Reaction-enhanced permeability during decarbonation of calcite + quartz → wollastonite + carbon dioxide: *Geology*, v. 28, p. 911–914, doi: 10.1130/0091-7613(2000)28<911:RPDDOC>2.0.CO;2.